Theoretical Chemical Dynamics: A Tool in Organic Chemistry

Dr. Xavier Chapuisat and Dr. Yves Jean

Laboratoire de Chimie Théorique*, Université de Paris XI – Centre d'Orsay, Faculté des Sciences, F-91405 Orsay, France

Contents

* The Laboratoire de Chimie Théorique is associated to the C. N. R. S. (ERA n°549).

Foreword

Obtaining the rate of a chemical reaction from the knowledge of the collisional elementary processes governing it, defines approximately the field of Chemical Dynamics. In most cases the investigation is restricted to molecular systems including a few atoms for the following reasons:

(i) the experiments for analyzing a flux of molecules in various intramolecular states are limited for technical reasons;

(ii) it is only in the case of small systems that "ab initio" potential energy surfaces can be computed over a wide range of coordinates where the dynamic can be studied rigorously.

The present article is a contribution for extending the scope of Chemical Dynamics in Organic Chemistry. In the first Chapter (A), previous trajectory studies in Chemical Dynamics are reviewed. The second Chapter (B) presents a general but elementary method for undertaking the dynamical study of any chemical reaction. This method seems to be applicable in a straightforward way to rather large molecular systems in Organic Chemistry. An application of this method is presented in the third Chapter (C): the optical and geometrical isomerizations of cyclopropane are treated dynamically[a]. It makes use of an ab initio potential energy surface[2-4]. The results are, as far as possible, compared with experimental results[b].

It should be emphasized that classical trajectories methods at present can be considered as fairly standard techniques for studying the dynamical behaviour of small molecular systems (either triatomic or tetraatomic). As a consequence many technical points have already been discussed in great detail in the literature[7-9] and they will not be discussed here. Such technical questions are, for instance:

(i) should a parameter defining an initial state be either scanned or sampled in a random way (Monte-Carlo methods)? ;

(ii) should the sampled points have uniform density or be distributed according to some weighting function?;

(iii) should quantized values of the initially observable quantities be exclusively selected? etc . . .

Other important topics related to the technology of trajectories will not be discussed either, for instance:

(iv) which integrator should be used to obtain the best compromise between stability and efficiency?[10-12];

(v) what are suitable tests to stop a trajectory integration according to the type of outcome produced?[7]

(vi) what type of semi-empirical potential should be preferentially used for a given reaction?[8] etc . . .

We will restrict this article to developing in detail our original contribution to the study of Chemical Dynamics in the field of Organic Chemistry. Consequently we will not say much about the connection between our work and semi-empirical statis-

---

a) This study was previously published in the Journal of the American Chemical Society[1,2].

b) More details on the subject can be found in our two "Thèses de Doctorat d'Etat": Yves Jean, Orsay (1973)[5] and Xavier Chapuisat, Orsay (1975)[6].

tical methods of chemical reactivity, such as the transition state method or the Rice-Ramsperger-Kassel-Marcus (RRKM) theory of unimolecular reactions[13–15]. The two points of view, dynamical and semi-empirical, differ greatly. Once again, the comparison is only meaningful in the case of small molecular systems for which complete and rigorous results have been obtained within both methodologies.

Finally, in view of all the restrictions above, the title of this article could as well be: "What can we do with trajectories in Organic Chemical Dynamics and under what kind of restrictions (drastic or not) is it possible?"

A. Trajectory Studies in Chemical Dynamics

1. Introduction

In this chapter we define the scope of this article, mention some studies relevant to it and give references where these studies are dealt with.

It is quite simple to say that this article deals with Chemical Dynamics. Unfortunately, the simplicity ends here. Indeed, although everybody feels that Chemical Dynamics lies somewhere between Chemical Kinetics and Molecular Dynamics, defining the boundaries between these different fields is generally based more on surmisal than on knowledge. The main difference between Chemical Kinetics and Chemical Dynamics is that the former is more empirical and the latter essentially mechanical. For this reason, in the present article we do not deal with the details of kinetic theories. These are reviewed excellently elsewhere[16–21]. The only basic idea which we retain is the reaction rate. Thus the purpose of Chemical Dynamics is to go beyond the definition of the reaction rate of Arrhenius (activation energy and frequency factor) for interpreting it in purely mechanical terms.

This field of research is subject to rapid expansion at present because the improvement of sophisticated experimental methods coincides with an increase of the computational possibilities for the theoretical investigation of both the mechanical study of the nuclear motion and the quantum mechanical study of the electron potential governing this motion.

The experimental situation has been the subject of several recent review papers, either general[22–24] or more specialized (molecular beams[25–32], infrared chemiluminescence[33], reactions of small molecules in excited states[34], etc . . .). The quantum mechanical theoretical approaches of Chemical Dynamics were also reviewed recently[8, 35, 36].

Since the scope of this article is purely theoretical, we just outline below the state of the experimental situation. The ideal experiment in Chemical Dynamics would be that in which starting with reactants in definite intramolecular quantum-states and running towards each other in a definite way (relative velocity and orbital angular momentum) the distribution of the products over the various intramolecular quantum-states and the state of the relative motion (direction and velocity) would be measured. Such an experiment would show whether there is a preferential molecular orientation at the heart of the collision, what the lifetime of the intermediate complex is, how the excess energy is distributed over the various degrees of freedom of

this complex, etc. . . Unfortunately, this experiment has not been carried out yet, but there are experiments which fulfill one part or the other of the ideal experiment. In crossed-molecular-beams experiments, the reactants are prepared in perfectly defined states[37–53]. For instance a laser can select a given rotation-vibration intramolecular state[54, 55]. The products are analyzed by means of one of the following techniques:

(i) the laser-induced fluorescence[56–58];
(ii) the infrared chemiluminescence[33, 59–63];
(iii) the electric resonance spectroscopy[64–67] and
(iv) the chemical laser[59, 68–74].

We do not insist on stating details of these experiments. Let us just mention the recent work of Herschbach and collaborators which is a very impressive achievement[75, 76]. These authors have studied, by means of molecular beams, the very details of "termolecular" reactions involving van der Wall's bonds among halogen molecules, such as:

$$\begin{aligned} Cl_2 \ldots Cl_2 + Br_2 \longrightarrow\ & (1)\ Cl_2 + 2\ BrCl; \\ & (2)\ BrCl \ldots Cl_2 + BrCl \text{ and} \\ & (3)\ Br_2 \ldots Cl_2 + Cl_2. \end{aligned}$$

In particular, to channel (1) and (2) mechanisms involving formations of the same cyclic six-center intermediate complex can be attributed whereas channel (3) only requires Br_2 to interact with the nearer Cl_2 molecule of the dimer within a noncyclic molecular conformation. Thus channel (3) dominates at low collision energies (< 9 kcal/mol), but declines rapidly at higher collision energies and becomes much less probable than collision-induced dissociation to form $Br_2 + 2\ Cl_2$, this applies also to both channels (1) and (2).

In Chemical Dynamics the direct comparison between experiments (more precise than simple kinetic measurements of reaction rates) and theoretical results is in general rather subtle. As far as we know, it has been restricted to reactions in which a halide is produced. The most studied reaction, both theoretically[77, 80] and experimentally[47, 48, 69, 81], is

$$F + D_2 \longrightarrow DF + D,$$

or its isotopic variants

$$F + H_2 \longrightarrow HF + H \text{ and}$$
$$F + HD \longrightarrow HF + D.$$

Thus the activation energy for the formation of DF is minimal when F and D_2 collide colinearly. At low collision energy most molecules DF are observed backwards, in vibrational states $v = 2$, 3 and 4, at weak total angular momentum, etc. . . All the theoretical studies of this reaction, but one[80], use classical trajectories.

2. Trajectory Studies of Small Molecular Systems

Since theoretical Chemical Dynamics resort practically to classical trajectories, we briefly review below some previous works in this field[c].

The first chemical reaction studied by means of classical trajectories was $H_2 + H \longrightarrow H + H_2$ within the *collinear collision model*[84–87]. This pioneering work states the following: For any system driven by a bent potential valley, the reaction proceeds through a gradual transformation of the collision energy into vibrational energy of the product molecule. The first 3-dimensional trajectories were for the same reaction[88]. Since then, much important work has been undertaken. For instance, the way in which an empirical modification of the potential modifies the reaction-probability, the intramolecular states of the products, the deflection angle, etc. . . all these were the subject of many studies[89–95] and also of a review article[96].

The first "a priori" study (by Karplus, Porter and Sharma) of a chemical reaction undertaken on a large scale was again for $H_2 + H$, described by a London-Eyring-Polanyi-Sato (LEPS)-type potential[97–100]. All the standard concepts and techniques were introduced for this investigation[101]: 3-dimensional model, restricting the intramolecular states of the reactants to quantized states, obtaining the reaction total cross-section[d] as a function of the collision energy and of the intramolecular states of the reactants by averaging over the impact parameter (pseudo-random Monte-Carlo method), integrating these cross-sections with the collision energy to obtain the *rate constant* of the reaction, etc. . .

The main results of this study are[101]:

(i) the total reaction cross section is an increasing function of the collision energy that rises smoothly from a threshold to an asymptotic value;

(ii) the zero-point vibrational energy of the molecule contributes to the energy required for reaction, but the rotational energy does not;

(iii) the reaction probability is a smoothly decreasing function of the impact parameter;

(iv) for temperatures between 300 °K and 3000 °K the theoretical rate constant can be expressed by the form $K(T) = AT^{\alpha} \exp\{-E^{\ddagger}/kT\}$ where A, $E^{\ddagger}$ and α ($\simeq 1.18$) are constants;

(v) there is no evidence of a long-lived intermediate complex.

The model was extended to the general atom-diatom exchange reaction $A + BC \longrightarrow AB + C$[102, 103], for which Polanyi and Wong studied in *3 dimensions* the relative influence of both initial translational energy and vibrational energy. This depends largely on the location of the top of the potential barrier, either along the approach coordinate (case I) or along the retreat coordinate (case II). In case I translation is more effective than vibration in promoting reaction. Moreover, at low collision energy, a major part of the available energy transforms into vibration of the product molecule (at higher collision energy this fraction decreases). In case II the opposite situation is observed: vibration is more effective than translation. Moreover, for low vibra-

---

c) There are several more detailed review articles on the subject[7–9, 82, 83].

d) The cross section of an elementary collision process is roughly a measure of the reaction efficiency of this process.

tional energy of the reactants only a small part of the available energy appears as vibration in the product (at higher vibrational energy this fraction increases). This confirms the conclusion obtained within the collinear collision model. In both cases I and II most product molecules are scattered backwards at low collision energy (the peak of the distribution shifts forward at increased reactant energy, even in case II for an increase of reactant vibration).

Then the Karplus *et al.* model was extended to more complex reactions[104, 105], such as

$$K + CH_3I \longrightarrow KI + CH_3$$ [92, 93, 99, 100, 106]

and finally to the general *thermal bimolecular* reaction in the gas-phase: $A + B \rightleftharpoons C + D$[107, 114]. For the latter it is possible to obtain the forms for the theoretical rate constants[19, 82, 101, 115–120] for the forward ($\vec{K}$) and the backward ($\overleftarrow{K}$) reactions [defined by[e]: $-d(A)/dt = \vec{K}(A)(B) - \overleftarrow{K}(C)(D)$] as functions of the temperature. If the gas phase is homogeneous the temperature is introduced through maxwellian distribution functions. The result is:

$$\vec{K} = \sum_{\chi_A, \chi_B, \chi_C, \chi_D} F_A(\chi_A) F_B(\chi_B) \int d\vec{v}_A F_A(\chi_A; \vec{v}_A) \int d\vec{v}_B F_B(\chi_B; \vec{v}_B)$$

$$v\, \sigma(\chi_A, \chi_B, \chi_C, \chi_D; E_{col})$$

$$\overleftarrow{K} = \sum_{\chi_A, \chi_B, \chi_C, \chi_D} F_C(\chi_C) F_D(\chi_D) \iint d\vec{v}_A\, d\vec{v}_B\, F_C(\chi_C; \vec{v}_C) F_D(\chi_D; \vec{v}_D)$$

$$v\, \sigma(\chi_A, \chi_B, \chi_C, \chi_D; E_{col})$$

where χ_I (I = A, B, C, D) denotes the set of all the quantum numbers defining the intramolecular state of molecule I (rotations and vibrations) $F_I(\chi_I)$ is the distribution function of the intramolecular quantum states of molecule I, $\vec{v}_I$ is the velocity of molecule I, $F_I(\chi_I; \vec{v}_I)$ is the normalized distribution function of the velocity of molecule I in the state χ_I, v is the initial relative velocity and E_{col} the collision energy:

$$v = |\vec{v}_A - \vec{v}_B| = (2E_{col}/\mu)^{1/2}$$

where μ is the reduced mass of A and B.

$$\sigma(\chi_A, \chi_B, \chi_C, \chi_D; E_{col})$$

is the reaction cross section of the elementary collision process $[A(\chi_A) + B(\chi_B) \longrightarrow C(\chi_C) + D(\chi_D)]$ at collision energy E_{col}. It is this quantity which is obtained by means of trajectories.

---

[e] This definition is for low concentrations and implies that the rate constants depend neither on the concentrations nor on the time.

This result is purely statistical. Replacing the distribution function by particular expressions, depending on the temperature, is the last operation[f]. When a dynamical process occurs the equilibrium distribution function (maxwellian) should be modified, and the greater the reaction rate compared to the relaxation rates of both the velocities and the intramolecular states, the greater the modification[121–123]. Thus it is only for low reaction rates that equilibrium distribution functions can be inserted in the formulas above, and that the reaction rate depends on the temperature, but neither on the time nor on the concentrations.

Now a question must be raised: which connection is there between classical trajectories results and results obtained through Quantum Mechanical calculations?

The Quantum Mechanical study of molecular collisions and of the chemical reaction is itself an important topic[124]. There are several review papers[35, 36, 125–129] and textbooks[130–139] on the subject. Unfortunately, there are no exact quantum results within a realistic model of a chemical reaction yet, not even for the simplest 3-atoms exchange. Thus the comparison is limited to particular cases.

For instance, $H + H_2 \longrightarrow H_2 + H$ was studied in 3-dimensions within a model where the vibrational states were reduced to a single one for each of the three possible product molecules[140]. At low collision energy (less than the classical energy threshold) the reaction cross section is non zero because of tunnelling. For the same reaction studied colinearly the following conclusions emerge[141–143]:

(i) for great values of the collision energies the quantum mechanical reaction probability slightly oscillates around the classical probability, because of the gradual "opening of excited vibrational states" in the products;

(ii) the reaction probability extends below the threshold by tunnelling. Thus, at low temperature and for the phenomenon of a pronounced quantum nature (such as the exchange of a light atom between two heavy groups), the classical trajectory reaction rate may be an underestimated approximation of the true reaction rate.

On the basis of such results and, more convincingly, on the strength of semiclassical investigations (classical S-matrix of Miller and Marcus[144–150]) it can be asserted that the classical description of the nuclear motion in the course of a molecular collision (either reactive or not) is not in itself a severe restriction. Thus, McCullough and Wyatt[151–152] have shown that for collinear $H + H_2 \rightarrow H_2 + H$ the agreement is quite good between the classical and the time-dependent quantum-mechanical descriptions during the greatest part of the reaction. A slight discrepancy appears only near the end of the reaction; the classical reaction is completed somewhat faster than the quantum-mechanical one. Nevertheless, all the dynamical effects such as the centrifugal force pushing the representative point of the reaction towards the outer part of the bent reaction valley and the whirlpool turbulence effects close to the saddle point, are surprisingly well described classically.

---

f) In the case of a complete equilibrium distribution, the result is:

$$K(T) = (8/\pi\mu kT)^{1/2}/kT \int_0^\infty dE_{col}\, \sigma'(E_{col})\, E_{col} \exp(-E_{col}/kT),$$

where: $\sigma'(E_{col}) = \sum_{x_A, x_B, x_C, x_D} F_A(x_A)\, F_B(x_B)\, \sigma(x_A, x_B, x_C, x_D; E_{col})$.

To wind up this chapter, we enumerate below the various fields of application of classical trajectories in Chemical Dynamics.

Many trajectories were integrated to obtain either total reaction cross sections for comparison with molecular beams experiments[79, 105, 153–171], or rotational and vibrational relaxation times of the products of chemical reactions, or intermolecular energy transfers[103, 107–111, 172–185], etc. . .

As seen previously, the chemical reactions studied most often are the exchange ones. Those requiring several potential energy surfaces of excited states (diabatic reactions) are worth special mention, since they most certainly define a domain of application with a future for classical trajectories. An electron jump from one surface to another requires either to be given a statistical probability of occurence by the Landau Zener formula[186, 187] (or one of its improved versions[188–192]) or to be described by means of complex-valued classical trajectories as a direct and gradual passage in the complex-valued extension of the potential surfaces (generalization of the classical S-matrix[193–197]).

Some atomic recombinations catalized by a rare gas atom[198–205] and some reactions involving a long-lived intermediate complex[112, 113, 206–208] were also studied classically. *Unimolecular* reactions are quite advantageous for trajectory studies since the potential is generally easy to express and the total energy is sufficiently great for reasonably neglecting the discreteness of vibrational levels of the reactant[7]. Until recently only triatomic decomposition has been studied extensively: $ABC \longrightarrow AB + C$[209–211]. The main concern is for the distribution of molecular lifetimes (the time elapsed before decomposition occurs) and for the variation of this distribution when varying the total energy and the particle mass. This can be compared directly with semiempirical predictions. Thus, it is well established for triatomic systems that the RRKM rate coefficients[13] satisfactorily agree with trajectory results. Another important advantage of trajectory methods is to provide the final energy partitioning between AB and C.

More recently, the unimolecular isomerization $CH_3NC \longrightarrow CH_3CN$ gave rise to elaborated studies by Bunker and collaborators[212–215]. The pressure dependence of the thermal reaction rate constant is well explained by the RRKM theory, applying the simple concept of the geometry and vibrations of the activated molecule[216]. However, the fact that the hot-atom displacement reactions

$$T^* + CH_3NC \longrightarrow CH_2TNC + H$$

and

$$T^* + CH_3CN \longrightarrow CH_2TCN + H$$

both result at the very end in CH_2TCN (observed by trajectories) is indicative of a failure of the RRKM theory for the unimolecular isomerization of nascent molecules[217]. In particular, CH_3NC is not a good RRKM molecule under non-thermal conditions, because the vibrational modes of CH_3NC are too far from being equally coupled to one another and also to the mode of isomerization. For unimolecular reactions it should be kept in mind that, since many vibrations (and not only the single translation) may play important roles, trajectory studies are always delicate and require much caution.

There have been a number of interesting trajectory studies of organic reactions that have used *empirical* potential energy surfaces. $CH_3NC \longrightarrow CH_3CN$ is the first example. The second example is

$K + C_2H_5I \longrightarrow KI + C_2H_5$ (studied by Raff)[218]

where the ethyl group is treated as a two-body system. The main results are:

(i) the total reaction cross section for this reaction is less than that for $K + CH_3I \longrightarrow KI + CH_3$, due to the increased steric hindrance;

(ii) KI is predominantly scattered backwards;

(iii) the C–C stretch of the ethyl absorbs an important part (15%) of the heat of reaction;

(iv) the reaction can occur by two mechanisms, either directly or through formation of a collision complex.

In the first mechanism most of the reaction energy transforms into rotation-vibration energy of KI, while in the second mechanism the energy distribution between the products is more random. A third example of organic reaction studied dynamically is that of a "hot" tritium atom on a methane molecule (studied by Polanyi and collaborators[219] on the one hand and by Bunker and collaborators[220–221] on the other hand). The main findings of several studies (using various potential energy surfaces) are:

(i) both abstraction of H by T ($T^* + CH_4 \longrightarrow TH + CH_3$) and T-for-H substitution ($T^* + CH_4 \longrightarrow H + CH_3T$) are direct (non complex) and concerted (non sequential) reactions;

(ii) substitution is favoured at intermediate collision energy (90–160 kcal/mol collision energy);

(iii) substitution with Walden inversion is an important fraction of overall substitution at low collision energy (40–100 kcal/mol);

(iv) the greatest part of the collision energy transforms into translational energy of the products;

(v) at 45–90 kcal/mol the product molecule is scattered sideways, following abstraction and backwards following substitution;

(vi) for abstraction, replacing T by D, the abstracted H by D, or CH_3 by a heavier radical results in a decrease of the reaction cross section;

(vii) for substitution, replacing T by D or the abstracted H by D results in a decrease of the reaction cross section while the latter increases when replacing CH_3 by a heavier radical.

We have kept the dynamical study of organic reactions by means of classical trajectories and based on semi-empirical and ab initio potential energy surfaces for the end. These studies are rare and constitute most likely a research subject with a future. The difficulty is to obtain forces acting on a large numbers of atoms. Constructing a potential whose partial derivatives provide reasonable forces is more and more difficult when the number of atoms and the directionality of valence forces increase[7, 9]. Except for the reaction study presented in the 3rd chapter of the present article, (in which an ab initio potential energy surface is interpolated and differentiated to give the forces) and as far as we know, these studies are reduced to a single one by Wang

and Karplus[222]. It deals with the insertion of singlet methylene into the hydrogen molecule:

$CH_2 + H_2 \longrightarrow CH_4$.

Here the forces are derived directly from matrices associated with SCF–MO calculations (at the semi-empirical $CNDO_2$ level). The results for the heat of reaction are accurate. The methylene is shown to be inserted into the hydrogen molecule for a wide range of initial conditions. But the most significant conclusion is that the analysis of the reaction in terms of the static reaction-path alone is largely insufficient, compared with the more realistic dynamical conclusions about the mechanism which is very complicated.

B. A General Framework for Chemical Dynamics in Organic Chemistry

The theoretical investigation of a chemical reaction is essentially a two-step study. The first step is *static.* It consists of computing the potential energy of the reaction system as a function of the different geometrical parameters. Hence, some information on the reaction mechanism can be obtained, such as

(i) the *minimum-energy path* to go from reactants to products and consequently the shape of the *reaction coordinate;*

(ii) the difference between the calculated energies for the reactants and for the system at the *transition state,* which is compared to the *activation energy* of the reaction as a first approximation. In recent years, the growth of scientific computers, as well as the realization of fast programs for quantum mechanical calculations has made the extensive investigation of potential-energy surfaces possible for many organic reactions involving rather complex molecules.

The second step is of a *dynamical* nature. It consists of obtaining dynamical trajectories on the potential surface. Classical Mechanics are supposed to describe correctly the atomic motion. In certain cases such a study, at the end, allows one to obtain the rate constant of the reaction[101]. In other respects the dynamical study brings new information on the mechanism of the reaction[102–103], which cannot be derived only from the study of the static potential surface. Moreover, the dynamical study is sometimes clearly indispensable for the elucidation of the reaction mechanism. Thus, the reaction $H_2 + I_2 \longrightarrow 2$ HI was considered for a long time to be a simple bimolecular reaction. Semi-empirical calculations of the potential-barrier height for a bimolecular process gave a result of 42 kcal/mol[179, 223], an excellent agreement with the experimental value of the activation energy (41 kcal/mol). However, dynamical trajectories calculations have shown that the mechanism is much more complicated than previously thought. In particular the conflict between two possible channels ($H_2 + I_2 \longrightarrow H_2 + 2\,I \longrightarrow I + H_2I$ (collinear) $\longrightarrow 2$ HI on the one hand[7, 224–226], and direct $H_2 + I_2 \longrightarrow 2$ HI on the other hand[227]) has not yet been resolved. Nevertheless, the dynamical study of the first channel gave reaction rates of recombination of $H_2 + 2\,I$ in good agreement with the experiment[228].

Complete dynamical studies, including the calculation of macroscopic reaction rates, have been restricted, until now, to small molecular systems[7, 9]. They require a preliminary knowledge of all the regions of the potential surface that are accessible for a given total energy. In addition, very many dynamical trajectories must be computed for suitably selected sets of initial conditions. For larger systems – even the smallest systems of interest in organic chemistry – it is impossible to obtain reaction rates by means of a complete dynamical study. Too many degrees of freedom have to be taken into account to obtain the full potential surface. Simplified assumptions are required to scan the surface. In general, only those geometrical parameters which contribute notably to the reaction path are varied. The secondary parameters are either held constant or varied in a conventional way. There is no choice but to carry these constraints over into the dynamical calculation. Then the system is said to be *constrained.* Consequently, the vibrational excitation of purely nonreactive modes is ignored. From a static point of view, this is not a severe restriction, if the important parameters have been carefully selected. On the contrary, from a dynamic point of view, the *a priori* neglect of any energy transfer between reactive and nonreactive modes (as well as the possible dissipation of a part of the energy over various nonreactive modes) can play a crucial role, in particular near the middle of the reaction where the final outcome of the reaction is decided.

Nevertheless, the dynamical study of the elementary processes occuring in the course of a reaction remains useful and complementary to the static study of the potential surface, even though it is incomplete and does not lead to the reaction rate. In particular, the comparison of dynamical trajectories with the static minimum-energy path is very instructive. As we mentioned in Chap. A for $CH_2 + H_2 \longrightarrow CH_4$[222], the initial conditions seem to play a crucial part in the shape of dynamical trajectories; only certain specific initial conditions lead to trajectories close to the minimum energy path; most dynamical trajectories are much more complex than this path. Furthermore, deviations may result from the fact that for a given potential surface in several dimensions the optimum path is most often drawn approximately under the assumption that the evolution of the system can be represented by the sliding of a mass point on the potential surface. This model is generally unsuitable for constrained systems[6, 19].

I. The Cubic Splines for Expression of the Potential Energy Functions

1. Introduction

Quantum chemical calculations provide the values of a multi-dimensional potential at the mesh points of a grid. Several coordinates are varied step by step and to each set of all these coordinates there is a corresponding number. However, we need a potential energy function which is analytic if possible, continuous and differentiable in any order. At the mesh points of the grid the values of this function are to be as close as possible to the computed ones. In addition, the values of the derivatives of this function with respect to any coordinate must be physically possible on the limiting contour surrounding the region of the potential surface studied. This is very im-

portant in order to avoid starting the numerical propagation of a trajectory the wrong way in a limiting region; after the propagation this would lead to an incorrect result in the opposite limiting region.

Different procedures can be envisaged. Most commonly used for small systems is a simple analytical formula which is derived from a physical basis[7–9]. Each parameter in such a formula has a specific physical meaning and can be optimized (for instance by a least squares fit). The main advantage of this procedure is that the parameters may be varied independently (this is the origin of many physical studies, see for instance Ref.[218]). But there are two drawbacks in doing this. Firstly, varying a parameter modifies the whole surface (for instance, modifying the height of a gaussian barrier at a constant parameter of steepness, implies a change in the width of the barrier). Secondly, in a strict sense, such a formula is hardly exact anywhere, since it is not an interpolation formula. However, this procedure is to be used as often as possible because of the high speed in computing the numerical values of simple expressions. We are not discussing here which analytical formula is the most suitable for a given molecular system. The treatment of these topics can be found in the literature[7, 9].

Many problems can be found in large systems in which most of the degrees of freedom are artificially frozen. Then the potential energy, as a function of the coordinates over a wide range, can become very complex. An alternative procedure is to use interpolation techniques. By the common polynomial techniques all the values of either the potential or its derivatives can be exactly fitted whenever it is necessary; but this leads to polynomials of a very high degree (hundreds of mesh points may have to be considered). Consequently, instabilities can appear, especially on the sides of the region studied (see Fig. 1 for a one dimensional case).

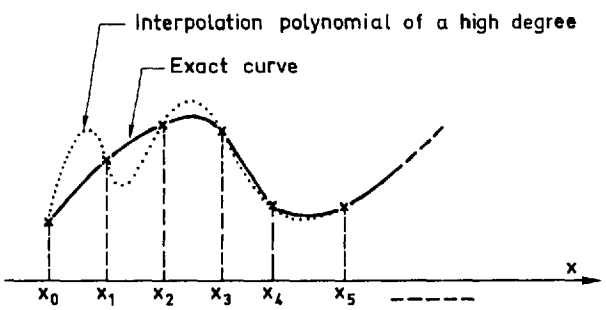

Fig. 1. An example of a possible behavior of an interpolation polynomial of high degree, as compared with the exact function. This is what we call an instability on the sides of the range of interpolation

Therefore, we must search for an analytical expression or the potential energy which exactly fits the calculated values at each mesh point of the grid, which avoids divergence on the sides of the physically interesting region and which has, nevertheless, a rather simple form. The aim of the present section is to use a procedure which

provides an expression fulfilling all these requirements by means of cubic spline functions[g].

In order to avoid any mathematical sophistication, we restrict ourselves to the construction of only those functions that are of interest in the application. Many more details can be found in the pioneering work of Ahlberg, Nilson and Walsh[233,234] and in various textbooks on the subject[235,236]. Some authors already applied spline techniques to various problems in Chemical Physics, either to interpolate ab initio potential surfaces[114,237,238] or experimental data[239] or to analytically expand atomic orbital functions[240–242] or to solve bound state Schrödinger equations[243].

2. One Dimensional Cubic Splines

On an interval $[x_{j-1}, x_j]$ of a variable x, there exists one cubic function $S_j(x)$ and only one such that:

$$\begin{aligned} &(1) \quad S_j(x_{j-1}) = y_{j-1} \text{ and } [dS_j(x)/dx]_{x_{j-1}} = m_{j-1}; \\ &(2) \quad S_j(x_j) \quad = y_j \quad \text{and } [dS_j(x)/dx]_{x_j} \quad = m_j. \end{aligned} \tag{1}$$

A convenient expression for this function is for instance:

$$S_j(x) = (\bar{y}_j - h_j M_j/8) + (3\,Y_j - h_j \bar{m}_j)\,X_j/2 + h_j M_j X_j^2/2 + 2\,(h_j \bar{m}_j - Y_j)\,X_j^3 \tag{2}$$

where: $X_j = (x - \bar{x}_j)/h_j$ lies within $[-1/2, +1/2]$

and: $\bar{x}_j = (x_j + x_{j-1})/2$, $\bar{y}_j = (y_j + y_{j-1})/2$, $\bar{m}_j = (m_j + m_{j-1})/2$,

$h_j = x_j - x_{j-1}$, $Y_j = y_j - y_{j-1}$, $M_j = m_j - m_{j-1}$.

Now we consider an interval $[a, b]$ of the variable x, which is subdivided by a mesh of points:

$$\Delta \equiv \{a = x_0 < x_1 < \ldots\ldots x_{N-1} < x_N = b\}.$$

We associate a set of ordinates with this set of abcissas;

$$y \equiv \{y_0, y_1 \ldots\ldots y_{N-1}, y_N\}$$

and with the extremal abcissas we associate two slopes: m_0 and m_N. We look for a function $S_\Delta(x)$, which is continuous on $[x_0, x_N]$ (as are its first and second derivatives), which coincides with a cubic in each $[x_{j-1}, x_j]$ and satisfies:

$$\begin{aligned} &S_\Delta(x_j) = y_j \quad (j = 0, 1 \ldots N) \\ &S'_\Delta(x_j) = m_j \quad (j = 0, N) \end{aligned} \tag{3}$$

---

g) An alternative analytical and stable interpolation technology has recently been extensively used: the continued fraction[194,195,229–232].

We call this function a cubic spline on Δ. The definition of such a function requires a knowledge of the intermediate slopes:

$$m_j = [dS_\Delta(x)/dx]_{x_j} \qquad (j = 1, 2 \ldots N-1)$$

From the continuity requirement imposed on $S''_\Delta(x)$ at x_j $(j = 1, 2 \ldots N-1)$ the set of linear equations results[2,3,4]:

$$\lambda_j m_{j-1} + 2\, m_j + \mu_j m_{j+1} = c_j \qquad (j = 1, 2 \ldots N-1) \tag{4}$$

where: $\lambda_j = h_{j+1}/(h_j + h_{j+1})$

$\mu_j = h_j/(h_j + h_{j+1}) = 1 - \lambda_j$

$c_j = 3\,\lambda_j (y_j - y_{j-1})/h_j + 3\,\mu_j (y_{j+1} - y_j)/h_{j+1}$

In matrix notation:

$$\begin{bmatrix} 2 & \mu_1 & 0 & \ldots 0 & 0 & 0 \\ \lambda_2 & 2 & \mu_2 & \ldots 0 & 0 & 0 \\ \vdots & \vdots & \vdots & \vdots & \vdots & \vdots \\ 0 & 0 & 0 & \ldots \lambda_{N-2} & 2 & \mu_{N-2} \\ 0 & 0 & 0 & \ldots 0 & \lambda_{N-1} & 2 \end{bmatrix} \times \begin{bmatrix} m_1 \\ m_2 \\ \vdots \\ m_{N-2} \\ m_{N-1} \end{bmatrix} = \begin{bmatrix} c_1 - \lambda_1 m_0 \\ c_2 \\ \vdots \\ c_{N-2} \\ c_{N-1} - \mu_{N-1} m_N \end{bmatrix} =$$

$$= \begin{bmatrix} \gamma_1 \\ \gamma_2 \\ \vdots \\ \gamma_{N-2} \\ \gamma_{N-1} \end{bmatrix} \tag{5}$$

Standard algorithms exist to solve such a band system in an efficient and stable way. The solution spline function $S_\Delta(x)$ exists and is unique. Moreover, it is an excellent interpolation function which converges to $f(x)$ when $N \to \infty$, if $\lim_{N\to\infty}(h_j) = 0$.

An important special case is that of equal intervals. Then, $\lambda_j = \mu_j = \frac{1}{2}$ $(j = 1, 2 \ldots N-1)$ and the matrix in Eq. (5) – which we then call $\underset{\sim}{B}$ – is easily inverted. The result is (see Table 1):

$$[\underset{\sim}{B}^{-1}]_{i,j} = (-1)^{i+j} B_{i-1}\, B_{N-j-1}/(2^{j-i} B_{N-1}) \quad (1 \leqslant i \leqslant j \leqslant N-1) \tag{6}$$

where:

$$B_n = [(1 + \sqrt{3}/2)^{n+1} - (1 - \sqrt{3}/2)^{n+1}]/\sqrt{3}$$

$\underset{\sim}{B}$ is symmetric with respect to its two diagonals. The same remains true for $\underset{\sim}{B}^{-1}$:

$$[\underset{\sim}{B}^{-1}]_{j,i} = [\underset{\sim}{B}^{-1}]_{i,j}$$

$$[\underset{\sim}{B}^{-1}]_{N-i-1,N-j-1} = [\underset{\sim}{B}^{-1}]_{i,j}$$

Table 1. $\underset{\sim}{B}^{-1}$ matrices in the case of equal intervals for $N = 4, 7, 10$ and $N \to \infty$. All of these matrices are symmetric with respect to their two diagonals so that only the upper quarter is reproduced here. In the case $N \to \infty$ ($\underset{\sim}{C}$), the upper half is reproduced. The infinite matrix is cut when the elements on each line parallel to the main diagonal have reached a constant value.
All the numbers in this table are given with a precision of 10^{-6}

$N = 4$

.535714	−.142857	.035714	
	.571429		

$N = 7$

.535898	−.143593	.038475	−.010306	.002748	−.000687
	.574373	−.153899	.041223	−.010993	
		.577121	−.154586		

$N = 10$

.535898	−.143594	.038476	−.010310	.002762	−.000740	.000198	−.000053	.000013
	.574374	−.153903	.041238	−.011050	.002961	−.000793	.000211	
		.577137	−.154643	.041436	−.011103	.002974		
			.577335	−.154696	.041450			
				.577348				

$N \to \infty$

.535898	−.143594	.038476	−.010310	.002762	−.000740	.000198	−.000053	.000014	−.000004	.000001	−	−	−
	.574374	−.153903	.041238	−.011050	.002961	−.000793	.000213	−.000057	.000015	−.000004	.000001	−	−
		.577137	−.154643	.041437	−.011103	.002975	−.000797	.000214	−.000057	.000015	−.000004	.000001	−
			.577335	−.154696	.041451	−.011107	.002976	−.000797	.000214	−.000057	.000015	−.000004	.000001
				.577349	−.154701	.041452	−.011107	.002976	−.000797	.000214	−.000057	.000015	−.000004
					.577350	−.154701	.041452	−.011107	.002976	−.000797	.000214	−.000057	.000015
						.577350	−.154701	.041452	−.011107	.002976	−.000797	.000214	−.000057

Let us define a new quantity: $\sigma = \sqrt{3} - 2 = -0.267949\ldots$ Then:

$$B_n = (1 + \sqrt{3}/2)^n\ (1 - \sigma^{2n})/\sqrt{3}$$

and:

$$[\underset{\sim}{B}^{-1}]_{i,j} = [(\sigma^{j-i} - \sigma^{j+i})/\sqrt{3}]\ (1 - \sigma^{2(N-j)})/(1 - \sigma^{2N})\quad (1 \leqslant i \leqslant j \leqslant N-1) \qquad (7)$$

We can now write down an explicit expression for the slope m_i at the ith mesh point of the grid ($i = 1, 2 \ldots N-1$):

$$m_i = (3/2\,h) \sum_{j=1}^{N-1} [\underset{\sim}{B}^{-1}]_{i,j}\,(y_{j+1} - y_{j-1}) - ([\underset{\sim}{B}^{-1}]_{i,1}\,m_0 + [B^{-1}]_{i,N-1}\,m_N)/2 \qquad (8)$$

It should be emphasized that the quantities $[\underset{\sim}{B}^{-1}]_{i,j}$ decrease rapidly as j departs from i. Only a few terms centered around x_i are to be kept in the sum, in Eq. (8).

We now study the equal intervals cubic spline function for $N \to \infty$. This limiting case is of general interest, since it affords a considerable simplification in the applications of the spline theory. $|\sigma|$ being less than 1, we have:

$$\underset{\sim}{C}_{i,j} = \lim_{N\to\infty} [\underset{\sim}{B}^{-1}]_{i,j} = (\sigma^{|j-i|} - \sigma^{j+i})/\sqrt{3} \quad (1 \leqslant i \text{ and } j \leqslant N-1) \qquad (9)$$

This is the current element of the infinite symmetric matrix $\underset{\sim}{C}$ (see Table 1), the elements of which decay rapidly apart from the diagonal and tend to be constant values on each line parallel to the diagonal. If this line is marked by k such that $|i - j| = k$, the limiting value for large i and j is:

$$\lim_{i\to\infty} \underset{\sim}{C}_{i,\,i\pm k} = \sigma^k/\sqrt{3} \qquad (10)$$

Thus, for sufficiently large i, the slope m_i can be expressed as:

$$m_i = (\sqrt{3}/2\,h) \sum_{k=-l}^{+l} \sigma^{|k|}\,(y_{i+k+1} - y_{i+k-1}) \qquad (11)$$

The integer constant l is defined according to the precision required.

3. Cardinal Splines

Let us introduce the cardinal splines. They are a set of $N + 3$ independent one-dimensional cubic splines $\{A_\Delta^{(k)}(x), k = 0, 1 \ldots N; B_\Delta^{(k)}(x), k = 0, N\}$ forming a complete basis on which to expand any cubic spline on Δ. We define them as follows:

$$A_\Delta^{(k)}(x_i) = \delta_{ik}\ \ (i = 0, 1 \ldots N) \text{ and } [dA_\Delta^{(k)}(x)/dx]_{x_i} = 0 \qquad (i = 0, N)\ (k = 0, 1 \ldots N);$$
$$B_\Delta^{(k)}(x_i) = 0 \quad (i = 0, 1 \ldots N) \text{ and } [dB_\Delta^{(k)}(x)/dx]_{x_i} = \delta_{ik} \quad (i = 0, N)\ (k = 0, N). \qquad (12)$$

δ_{ik} is the Kronecker delta.

It is readily verified that the spline function defined by the set of conditions (3) can be expanded in the form:

$$S_\Delta(x) = \sum_{j=0}^{N} y_j A_\Delta^{(j)}(x) + m_0 B_\Delta^{(0)}(x) + m_N B_\Delta^{(N)}(x) \tag{13}$$

This expansion will be of great interest in the following.

In the case of equal intervals the slopes of the cardinal splines at the mesh points have a simple form; from Eq. (8) ($i = 1, 2 \ldots N-1$):

$$m_i \{A_\Delta^{(k)}(x)\} = (3/2\,h)([\underset{\sim}{B}^{-1}]_{i,k-1} - [\underset{\sim}{B}^{-1}]_{i,k+1}) \quad (k = 2, 3 \ldots N-2) \tag{14}$$

For $k = 0, 1, N-1$ or N this relationship is still valid under the condition that the $[\underset{\sim}{B}^{-1}]_{i,j}$ that do not exist (*i.e.* $[\underset{\sim}{B}^{-1}]_{i,-1}$, $[\underset{\sim}{B}^{-1}]_{i,0}$, $[\underset{\sim}{B}^{-1}]_{i,N}$ and $[\underset{\sim}{B}^{-1}]_{i,N+1}$) are regarded as being equal to zero. In addition:

$$m_i \{B_\Delta^{(0)}(x)\} = -[\underset{\sim}{B}^{-1}]_{i,1}/2 \text{ and } m_i \{B_\Delta^{(N)}(x)\} = -[\underset{\sim}{B}^{-1}]_{i,N-1}/2 \tag{15}$$

From the expressions (1), (7), (14) and (15) one deduces the following properties of the cardinal splines: (1) the cardinal splines $A_\Delta^{(k)}(x)$ and $A_\Delta^{(N-k)}(x)$ are mutually symmetric with respect to the center of the range Δ; (2) the cardinal splines $B_\Delta^{(0)}(x)$ and $B_\Delta^{(N)}(x)$ are antisymmetric; (3) The A-type cardinal splines are oscillating functions with a peak just a bit greater than 1 for a value of x very close to x_k (or rigorously equal to 1 at $x = x_k$ for the case of symmetric function) which rapidly damp out for the values of x apart from x_k; (4) the B-type cardinal splines are oscillating functions with a peak close to the middle of the end interval and which rapidly damp out away from that interval; (5) The absolute values of the cardinal splines

$$A_\Delta^{(k)}\left(\frac{x}{h}\right) \quad (k = 0, 1 \ldots N)$$

do not depend on h; (6) The absolute values of the cardinal splines $B_\Delta^{(k)}\left(\frac{x}{h}\right)$ ($k = 0$, N) are proportional to h.

In the case $N \to \infty$, the B-type cardinal splines can be considered to vanish unless x is close to $x_0 \cdot x_0$ however, can always be removed far from the range of x, which is of interest. In other words, whenever h is reduced (tends to zero), the two terminal terms in the r.h.s. of Eq. (13) become negligible compared with the first one, because of the properties (5) and (6) above. Moreover, the complete set of the A-type cardinal splines reduces to a unique symmetric function called $A_\infty(X)$; this function is to be translated ($hX = x - x_k$), in such a way that it possesses the maximum of unit height at $x = x_k$ in order that it may represent $A_\infty^{(k)}(x)$. The intermediate slopes characterizing this unique function are evaluated using Eq. (11):

$$\begin{aligned} m_{i-k} &= m_i \{A_{N\to\infty}^{(k)}(x) = A_\infty((x - x_k)/h)\} \\ &= (\sqrt{3}/2\,h)(\sigma^{|i-k+1|} - \sigma^{|i-k-1|}) = \alpha_{i-k}/h \end{aligned} \tag{16}$$

Table 2. To obtain the intermediate slopes characterizing the function $A_\infty(X)$, where $X = \frac{|x - x_k|}{h}$, the integer indices and values given here are to be inserted in the formula:

$[m\{A_\infty(X)\}]_{X=i} = \frac{\alpha_i}{h}$, where $\alpha_{-i} = -\alpha_i$

Otherwise: $\beta_i = \alpha_i + \alpha_{i-1}$ and $\gamma_i = \alpha_i - \alpha_{i-1}$

Hence: $\beta_{1-i} = -\beta_i$ and $\gamma_{1-i} = \gamma_i$

i	0	± 1	± 2	± 3	± 4	± 5	± 6	± 7	± 8	± 9	± 10	± 11
α_i	.0	∓.803847	±.215391	∓.057714	±.015465	∓.004143	±.001110	∓.000299	±.000080	∓.000021	±.000006	∓.000002
β_i	+.803847	−.803847	−.588456	+.157677	−.042249	+.011322	−.003033	+.000811	−.000219	+.000059	−.000015	+.000004
		+.588456	−.157677	+.042249	−.011322	+.003033	−.000811	+.000219	−.000059	+.000015	−.000004	+.000002
γ_i	−.803847	−.803847	+1.019238	−.273105	+.073179	−.019608	+.005253	−.001409	+.000379	−.000101	+.000027	−.000008
		+1.019238	−.273105	+.073179	−.019608	+.005253	−.001409	+.000379	−.000101	+.000027	−.000008	+.000002

The α's are given in Table 2. The function A_∞ is drawn in Fig. 2. Consequently, the spline expression of any function defined by a sufficiently large set of values $\{y_i\}$ regularly spaced, is now very simple:

$$S_{N\to\infty}(x) = \sum_j y_j A_\infty(|x - x_j|/h) \tag{17}$$

The sum is to be limited to a few terms, depending on the precision desired. This only presupposes that one knows the accurate values of y_j that are sufficiently far away from the x considered. From Fig. 2 one sees that four steps further away suffice since $A_\infty(X)$ is negligible, for $|X| > 4$, within 0.25% (for $|X| > 5$, within 0.09%).

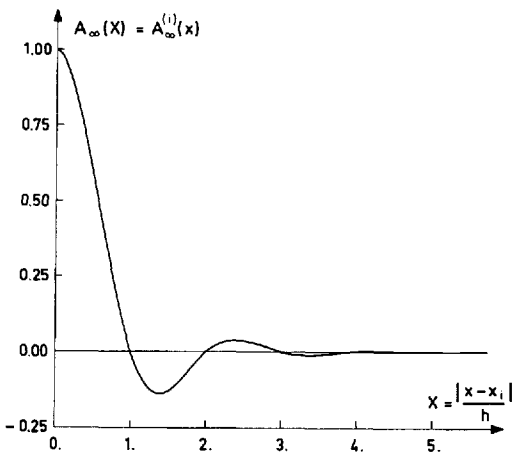

Fig. 2. The $A_\infty(X)$ function. $A_\infty\left(\frac{|x - x_k|}{h}\right)$ is the same as $A_\infty^{(k)}(x)$

Generalizing the one dimensional spline theory in relation to the two dimensional case is very straightforward. The explicit expressions of the multidimensional splines are beyond the scope of the present article. They can be found in the literature[2 3 4)] and have been used by one of us previously[1, 5, 6, 24 4)].

4. Supplementary Indications for Practical Uses

a) Reduction to the Case of Equal Intervals. We know a function $y(x)$ by the data set: $\{\tilde{x}_i$ and $\tilde{y}_i$ $(i = 0, 1 \ldots N); \tilde{m}_i$ $(i = 0, N)\}$, where the $\tilde{x}_i$'s are irregularly distributed. We define Δ, the mesh of regularly spaced abscissas: $\{x_i = \tilde{x}_0 + i(\tilde{x}_N - \tilde{x}_0)/N$ $(i = 0, 1 \ldots N)\}$. We reorder the expression of the spline – which is unique on $[x_0, x_N]$ – in the following way:

$$\sum_{i=1}^{N-1} y_i A_\Delta^{(i)}(x) = S(x) - [\tilde{y}_0 A_\Delta^{(0)}(x) + \tilde{y}_N A_\Delta^{(N)}(x) + \tilde{m}_0 B_\Delta^{(0)}(x) + \tilde{m}_N B_\Delta^{(N)}(x)] \tag{18}$$

Here the y_i's are $(N-1)$ unknowns, which are obtainable by imposing the $N-1$ conditions that $S(\tilde{x}_i) = \tilde{y}_i$ $(i = 1, 2 \ldots N-1)$ and then resolving a linear system of equations. The above reduction is of importance because of the high stability and simplicity of the cardinal splines on a mesh of regularly spaced abscissas.

b) Differentiation[234]. The flexibility of spline functions is very useful in the field of differentiation. Noting $\tilde{m}_j$ the average slope over the jth interval: $\tilde{m}_j = (y_j - y_{j-1})/h_j$ and $\underset{\sim}{W}$ the matrix in Eq. (5), after reordering the current derivative m_i is expressed as:

$$m_i = \lambda_1 [\underset{\sim}{W}^{-1}]_{i,1} (3\,\tilde{m}_1 - m_0) + 3 \sum_{j=2}^{N-1} \tilde{m}_j (\lambda_j [\underset{\sim}{W}^{-1}]_{i,j} + \mu_{j-1} [\underset{\sim}{W}^{-1}]_{i,j-1})$$
$$+ \mu_{N-1} [\underset{\sim}{W}^{-1}]_{i,N-1} (3\,\tilde{m}_N - m_N) \qquad (i = 1, 2 \ldots N-1) \qquad (19)$$

The structure of this formula is interesting. The λ's and μ's lying by definition between 0 and 1, $\underset{\sim}{W}$ is a band matrix with a dominant diagonal ($W_{i,i} = 2$). The same is approximately true for $\underset{\sim}{W}^{-1}$ ($[W^{-1}]_{i,i}$ close to 0.5). This shows that the m_i's are refinements of the $\tilde{m}_i$'s.

Now, from Eq. (2) we have $(x_{j-1} \leqslant x \leqslant x_j)$:

$$dS(x)/dx = (3\,\tilde{m}_j - \bar{m}_j)/2 + M_j X_j + 6\,(\bar{m}_j - \tilde{m}_j)\,X_j^2 \qquad (20)$$

(remember that: $\bar{m}_j = (m_j + m_{j-1})/2$ and $M_j = m_j - m_{j-1}$). Near to the center of the interval $\{S'(\bar{x}_j) = (3\,\tilde{m}_i - \bar{m}_j)/2\}$, it is noticeable that the derivative depends three times as much on the given quantity $\tilde{m}_j$ (directly related to the data) than on the computed one $\bar{m}_j$.

c) The Cubic Spline Functions in Classical Dynamical Studies. Consider a molecular system as a mechanical system to which no limitation to the free motion is imposed (symmetries excepted), i.e. no bond and no angle are frozen. Then the hamiltonian is expressed as:

$$H = T(P) + V(Q) \qquad (21)$$

where Q and P are two sets of suitable dynamical variables (respectively, coordinates and conjugate momenta) and the kinetic energy is:

$$T(P) = (\sum_k P_k^2/\mu_k)/2 \qquad (22)$$

μ_k is the mass associated with the coordinate Q_k. The first type hamiltonian equations of motion are simple:

$$\dot{Q}_1 = \partial H/\partial P_1 = \partial T/\partial P_1 = P_1/\mu_1 \qquad (23)$$

The second type equations:

$$\dot{P}_1 = -\partial H/\partial Q_1 = -\partial V/\partial Q_1 \qquad (24)$$

are generally more difficult to obtain, because the potential energy is a function of natural coordinates $x, y \ldots u \ldots$:

$$V(Q) = \mathrm{V}(x, y \ldots u \ldots) \tag{25}$$

where $x = x(Q), y = y(Q), \ldots u = u(Q) \ldots$

Thus the chain rule is used:

$$\dot{P}_1 = -(\partial \mathrm{V}/\partial x)(\partial x/\partial Q_1) - (\partial \mathrm{V}/\partial y)(\partial y/\partial Q_1) \ldots\ldots -(\partial \mathrm{V}/\partial u)(\partial u/\partial Q_1) \ldots\ldots \tag{26}$$

Suppose now, that the potential V is spline fitted[h]. We consider the general polydimensional case and that the number of mesh points in all directions are equivalent to infinity ($N \to \infty$). This situation is always attainable from a polydimensional grid of computed values in a sufficient quantity by subdivision of the step in each direction and preliminary interpolation of purely numerical supplementary values to be used in the spline expression, which therefore is:

$$\mathrm{U}(x, y \ldots u \ldots) = \sum_{i,j,\ldots n \ldots} \mathrm{V}_{i,j \ldots n \ldots} A_\infty[(x - x_i)/h_x] A_\infty[(y - y_j)/h_y] \ldots\ldots$$
$$A_\infty[(u - u_n)/h_u] \ldots\ldots \tag{27}$$

The partial derivatives required by Eq. (26) then are very simply expressed for instance:

$$\partial \mathrm{U}/\partial u = \sum_{i,j,\ldots n \ldots} \mathrm{V}_{i,j,\ldots n \ldots} A_\infty[(x - x_i)/h_x] A_\infty[(y - y_j)/h_y] \ldots\ldots$$
$$dA_\infty[(u - u_n)/h_u]/du \ldots\ldots \tag{28}$$

where, if $\mathrm{u}_{q-1} \leqslant \mathrm{u} \leqslant \mathrm{u}_q$:

$$dA_\infty[(u - u_n)/h_u]/du = [3\,\delta^*_{q-n}(1/2 - 2\,U_q^2) + \beta_{q-n}(3\,U_q^2 - 1/4) + \gamma_{q-n}U_q]/h_u \tag{29}$$

and: $\beta_k = \alpha_k + \alpha_{k-1}$, $\gamma_k = \alpha_k - \alpha_{k-1}$ and $\delta^*_k = \begin{cases} 1 \text{ if } k = 0 \\ -1 \text{ if } k = 1 \\ 0 \text{ otherwise} \end{cases}$

The local variable $U_q = \dfrac{u - \bar{u}_q}{h_u}$ lies within the limits $-\dfrac{1}{2}$ and $+\dfrac{1}{2}$. Values of β's and γ's are given in Table 2.

The algorithm is readily programmed. It allows for dynamical studies with non empirical potentials whatever the dimensionality of the problem under consideration.

---

h) In the two-dimensional case, McLaughlin and Thompson[114] recently used an elegant and convenient matrical method given by Jordan and de Boor[245].

5. Conclusion

The advantages of the spline functions as an interpolation technique are essentially threefold:

(1) they are general and directly related to the results of quantum chemistry calculations as they are produced by the specialists (grids of numerical values);

(2) the obtained potential energy surface can be modified locally without noticeably changing the rest of the surface. This allows for a great flexibility in the course of studies on the influence of local potential properties on whatever phenomenon is dependent on them;

(3) their flexibility makes them a tool with a future in the field of dynamical studies in theoretical chemistry.

The drawback of the method is that one does not obtain parameters that are of significance to the whole surface. To wind up this section, let us assert that the first application has shown the spline technique to be useful and advantageous[1, 2, 114, 244].

II. A Formulation of Classical Mechanics for Constrained Molecular Systems in Chemical Dynamics

1. Introduction

On generally restricts a Chemical Dynamics study to the framework of Classical Mechanics[7, 9, 82, 83, 246]. This is quite justified as long as no trajectory passes close to a crossing point or to a symmetry-avoided-crossing point[i) 247, 248] (the range of validity of classical trajectory studies can be extended to this last case by specific devices[186, 193–197, 246]). At the present time all the Classical Chemical Dynamics studies using adiabatic surfaces have been restricted to small molecular systems (including no more than six atoms)[7, 9, 104, 112, 222]. Indeed, a realistic dynamical study of a greater system is not a straightforward matter. In particular, the usual formulation of Classical Mechanics is relevant to mass points interacting through forces. For nuclear motion this formulation is well adapted to systems in which all the intramolecular degrees of freedom (plus the degrees of relative motion in the case of bimolecular encounters) are explicitly taken into account and therefore may change in the course of the motion. Such a system is called a *free system*. The inclusion of overall rotation, *i.e.* three supplementary degrees of freedom, is optional. Unfortunately, most studies in Chemistry concern systems in which the atoms are too numerous to allow a complete investigation of the entire potential energy surface. Thus many degrees of freedom must be held constant. For instance, some bond lengths which are not sensibly modified in the course of the reaction are fixed *a priori*.

---

i) Classical Mechanics is known to hold for the description of nuclear motions on a static potential surface from various semiclassical investigations[144, 148–150] and from direct comparison with quantum-mechanical results for small systems[140, 141, 143].

Similarly, when the atoms in a substituent group (an alkyl group for instance) do not participate in a reaction as individuals but only as a group, the geometry of the group is frozen. Such systems will be referred to as *constrained systems*, and we search for a suitable formulation of Classical Mechanics for them.

Indeed, the mechanical counterpart to a constrained system is a set of solids (frozen groups) articulated with each other through idealized hinges. The motion of the solids is driven by forces which derive from a potential depending on the remaining degrees of freedom. Below we present a method which executes the required job by introducing a matrix called the *constraint matrix*. This constraint matrix is built up with the mass like-coefficients appearing in the non-diagonal kinetic energy. It depends on generalized coordinates only, *i.e.* not on conjugate momenta. The equations of motion are simply obtained by inverting the matrix and by differentiating its elements with respect to generalized coordinates.

2. Classical Mechanics of Constrained Systems within Lagrangian and Hamiltonian Formalisms

We consider an N-particle mechanical system. A set of K constraints applied to it is holonomic[250] whenever all the relationships connecting the natural coordinates $\{Q_i, i = 1, 2 \ldots 3N\}$ of the particles in the system plus the time t – and which are a mathematical counterpart to the existence of constraints inside the system – are of the form:

$$g_l(Q_1, Q_2 \ldots Q_{3N}, t) = 0 \qquad (l = 1, 2 \ldots K) \tag{30}$$

The elimination of K dependent coordinates results in the introduction of a set of generalized coordinates $\{q_j, j = 1, 2 \ldots n\}$ where $n = 3N - K$, in terms of which the natural coordinates are expressed parametrically[j]:

$$Q_i = Q_i(q_1, q_2 \ldots q_n, t) = Q_i(q, t) \qquad (i = 1, 2 \ldots 3N) \tag{31}$$

Any conservative mechanical system which is either free or subject to holonomic constraints and whose potential does not depend on the generalized velocities is described by standard equations of motion (either Lagrangian or Hamiltonian).

The kinetic energy of the N-particle system is:

$$T = \frac{1}{2} \sum_{i=1}^{N} m_i (\dot{x}_i^2 + \dot{y}_i^2 + \dot{z}_i^2) \tag{32}$$

where x, y and z are cartesian coordinates. The introduction of $3N$ "natural" coordinates:

---

j) On the scale of molecules, all the constraints to be taken into account are mathematically idealized and of the holonomic type. Moreover, the defining transformation Eq. (31) do not depend on time explicitly.

$$Q_1 = m_1^{1/2} x_1,\ Q_2 = m_1^{1/2} y_1, \ldots\ldots\ Q_{3N} = m_N^{1/2} z_N \tag{33}$$

results in a simplified expression for T:

$$T = \frac{1}{2} \sum_{i=1}^{3N} \dot{Q}_i^2 \tag{34}$$

Then the natural coordinates Q_i ($i = 1, 2 \ldots 3N$) are expressed as functions of the independent generalized coordinates q_j ($j = 1, 2 \ldots n$). As an immediate consequence the analytical expression of the potential V is modified:

$$V(Q) = \mathrm{U}(q) \tag{35}$$

The natural velocity $\dot{Q}_i$ (the total differential of Q_i with respect to time) is:

$$\dot{Q}_i = \sum_{j=1}^{n} \frac{\partial Q_i(q)}{\partial q_j} \dot{q}_j \qquad (i = 1, 2 \ldots 3N) \tag{36}$$

Insertion of (36) into (34) provides the expression of the kinetic energy in terms of generalized coordinates:

$$T(q, \dot{q}) = \frac{1}{2} \sum_{j,k=1}^{n} A_{jk}(q)\, \dot{q}_j\, \dot{q}_k \tag{37}$$

where:

$$A_{jk}(q) = \sum_{i=1}^{3N} \frac{\partial Q_i(q)}{\partial q_j} \frac{\partial Q_i(q)}{\partial q_k} \tag{38}$$

$A_{jk}(q)$ is the current element of a matrix $\underset{\sim}{A}(q)$ called the *constraint-matrix*. $\underset{\sim}{A}(q)$ is a real symmetric matrix whose diagonal elements are positive; it depends on the generalized coordinates as variables and parametrically on the constraints. This matrix possesses an inverse since $\det \underset{\sim}{A}(q) = 0$ is not possible; it would correspond to a supplementary relationship between the coordinates only, *i.e.* a supplementary holonomic constraint.

The expressions of the generalized momenta in terms of the generalized velocities are:

$$p_i = \sum_{k=1}^{n} A_{ik}(q)\, \dot{q}_k \qquad (i = 1, 2 \ldots n) \tag{39}$$

The inversion of the matrix $\underset{\sim}{A}(q)$ results in:

$$\dot{q}_i = \sum_{k=1}^{n} A_{ik}^{-1}(q)\, p_k \qquad (i = 1, 2 \ldots n) \tag{40}$$

which is a convenient form of the Hamilton equations of the first type for constrained systems.

Insertion of Eq. (40) into Eq. (37) leads to the expression of the kinetic energy in terms of generalized coordinates and momenta:

$$T(q, p) = \frac{1}{2} \sum_{i,j=1}^{n} A_{ij}^{-1}(q)\, p_i p_j \tag{41}$$

$\underset{\sim}{A}^{-1}(q)$ exists; moreover, it is real and symmetric. It is important to note that obtaining $T(q, p)$ is no more difficult than an inversion of $\underset{\sim}{A}(q)$. The Hamilton equations of motion of the second type then are:

$$\dot{p}_i = -\frac{1}{2} \sum_{j,k=1}^{n} \frac{\partial A_{jk}^{-1}(q)}{\partial q_i} p_j p_k - \frac{\partial \mathcal{U}(q)}{\partial q_i} \quad (i = 1, 2 \ldots n) \tag{42}$$

since $H(q, p) = T(q, p) + \mathcal{U}(q)$.

On the basis of Eqs. (40) and (42), one may state that – once the constraint matrix $\underset{\sim}{A}(q)$ is known – using the hamiltonian formalism to study the dynamics of a constrained system amounts to

(i) inverting $\underset{\sim}{A}(q)$ and

(ii) obtaining the partial derivatives of all the elements of $\underset{\sim}{A}^{-1}(q)$ with respect to all generalized coordinates.

The Lagrange equations of motion are:

$$\sum_{j=1}^{n} A_{ij}(q)\, \ddot{q}_j = \sum_{k,l=1}^{n} \left[\frac{1}{2} \frac{\partial A_{kl}(q)}{\partial q_i} - \frac{\partial A_{ik}(q)}{\partial q_l} \right] \dot{q}_k \dot{q}_l - \frac{\partial \mathcal{U}(q)}{\partial q_i} \tag{43}$$

$$(i = 1, 2 \ldots n)$$

since $L(q, \dot{q}) = T(q, \dot{q}) - \mathcal{U}(q)$.

In order to solve numerically this set of coupled second order differential equations, it is generally the practice to use numerical integrators adapted to coupled first order differential equations only and, consequently, Eq. (43) must be transformed into:

$$\dot{q}_i = \pi_i \tag{44}$$

$$\dot{\pi}_i = -\sum_{j=1}^{n} A_{ij}^{-1}(q) \left[\sum_{k,l=1}^{n} \left(\frac{\partial A_{jk}(q)}{\partial q_l} - \frac{1}{2} \frac{\partial A_{kl}(q)}{\partial q_j} \right) \pi_k \pi_l + \frac{\partial \mathcal{U}(q)}{\partial q_j} \right] \tag{45}$$

$$(i = 1, 2 \ldots n)$$

It should be noticed that the bracket in Eq. (45) is independent of i and depends on j only. Using the Lagrangian formalism to study the dynamics of a constrained system amounts to

(i) inverting $\underset{\sim}{A}(q)$ and

(ii) obtaining the partial derivatives of all the elements of $\underset{\sim}{A}(q)$ with respect to all generalized coordinates.

3. Discussion

At this stage, we must stress one point: the more constrained the system, the smaller the dimension of the reduced problem and the more involved the matrix elements $A_{ij}(q)$. In other words, the reduction of a great number of natural degrees of freedom to a small number of privileged ones by imposing constraints to the system – which results in a shortening of quantum chemical calculations and a simplification of the potential energy surface – happens to introduce supplementary intricacies when dealing with dynamical problems. However, the requirement that a system retains the same symmetry along a reaction path does not appear as a constraint, although it is a restriction to free motion. In fact, a symmetry-constrained system can always be viewed as a free system with a smaller number of dimensions.

Now a qualitative distinction between two classes of constrained systems is discussed. The first class corresponds to a highly constrained system, that is to say a molecule in which at least two frozen groups of atoms are related by means of a hinge located at the atom in common with the two groups. Nothing more than what is in strict conformity with the general treatment presented above can be said for such a system. A preliminary difficulty is generally to express the constraints in a convenient way. A simple solution is to take as generalized coordinates those degrees of freedom that are of physical interest on the basis of either experimental or theoretical information. Expressing the cartesian and natural coordinates as functions of the generalized coordinates results in trigonometrical calculations. An important point is then to ascertain the fixity of the center of mass and, if necessary, the zero value of the total angular momentum. The last operation consists in applying the standard procedure exposed in paragraph 2. The whole work can be very long but is always feasible[1, 2].

The second class includes the minimally constrained systems, *i.e.* molecular systems in which certain groups are still frozen but are individually treated as solids interacting only through a position dependent potential. A quite simple example in this category is a rigid diatomic rotor moving in an external static field. For such systems, mechanical developments that are not possible in the general treatment can often be achieved[170].

Finally, the advantages of respectively, the Lagrangian and Hamiltonian methods, are compared below. Two points should be emphasized:

(i) the Hamiltonian equations are more balanced that the Lagrangian equations. Indeed, there appears a simple summation in Eq. (40) and a double one in Eq. (42) whereas, in Eq. (45) the summation in the expression of $\dot{\pi}_i$ is a triple one. Consequently, the numerical integration (by means of usual integrators) of Hamiltonian equations is somewhat faster and more stable than the integration of Lagrangian equations;

(ii) obtaining Hamiltonian equations requires differentiation of the matrix $\underset{\sim}{A}^{-1}(q)$ whereas, for Lagrangian equations, it is $\underset{\sim}{A}(q)$ which is differentiated. Since the matrix elements $A_{ij}(q)$ are often rather complicated, the matrix-elements $A_{ij}^{-1}(q)$ are even more complicated and their differentiation can result in very large and intricate expressions. Consequently, for highly constrained system, the Lagrangian integration often appears more suitable. The definitive choice for either one method or the other depends in fact on the particular system treated.

4. Conclusion

The present method is applicable to large constrained molecular systems in a streightforward way. Its main advantage is to allow the direct resolution of dynamical problems in those generalized coordinates in terms of which the potential energy functions are expressed, obtained through quantum-chemical calculations. Its main drawback is that the derivation of the analytical constraint-matrix can be quite tedious in some intricate cases of highly constrained systems. The illustration of such a case is presented in the next chapter. To wind this formal section up, let us mention that an alternative technique to resolve mechanical problems involving constrained systems is that of the Lagrange multipliers[k].

III. Some Remarks on How to Select Initial Conditions

1. Introduction

To start the mathematical integration of the equations of motion for one particular trajectory, a set of initial values of coordinates and either velocities or momenta must be specified. These, however, are dependent on the experimental conditions which need be reproduced, such as collision energy, intramolecular vibrational energies etc. . . In addition, some other variables, for instance intramolecular instantaneous elongations, molecular orientations, impact parameter, etc. . ., are necessarily specified in classical mechanics but are not observable microscopically because of the Uncertainty Principle. The ensemble of these result in a set of trajectories associated with a given set of observable initial conditions.

Many trajectories are necessary to describe all the different events that are summed up to form a unique wave describing the global chemical reaction under observable conditions in quantum mechanics. In this respect, a set of classical trajectories which spread around a mean trajectory in classical mechanics corresponds roughly to the quantum mechanical spreading (through space or time) of the density probability function around its center.

Since the number of trajectories is necessarily limited (in particular when computing the forces requires a great amount of computer time), good criteria for selecting the initial conditions are of prime interest. The problem is so important that it was discussed at length several times before[7, 101]. In this section we just consider what can be done in the case of constrained systems. The approximation of the "constraints" is so rough as to eliminate the need for any of the refined corrections that allowed to get very accurate results for small free molecular systems (cf. Chapter A).

Several domains of application need to be distinguished. In the thermal chemistry of unimolecular reactions, a complex process, which is not known to us, leads to the

---

k) By the Lagrange multipliers technique[250] the differential equations are integrated in the natural coordinates and the Lagrange multipliers are used to keep constant the constraints at each step of integration.

initial energy of the reacting molecule (activated molecule). All the possible sets of initial conditions should therefore be studied in order to determine which sets of those initial conditions favour the reaction. To have a statistic weight for each set of initial conditions is desirable but not always possible to obtain. In photochemistry the intramolecular activation energy originates through a photon impact, *i.e.* a well-defined and instantaneous process. From a knowledge of the Franck-Condon principle, it is possible to ascribe to each individual trajectory a statistical weight[189, 191] from which average values of different quantities can be derived.

In the thermal chemistry of bimolecular reactions studied within the framework of trajectories calculations, it is normally possible to obtain the rate constant of the reaction as a function of temperature[116] (cf. Chapter A). However, this can require rather tedious calculations, because of the necessity of averaging the results over a large distribution of individual trajectories. We do not discuss further the problem of bimolecular reactions.

2. Physical Observables and Phase Variables

At the beginning of any trajectory one must specify either the coordinates and the velocities $[q_0, \dot{q}_0]$ or the coordinates and the momenta $[q_0, p_0]$. It is physically desirable that the initial conditions describe an observable situation of the reactants. We denote by G the set of all the experimentally observable quantities (called *physical observables*) which must be reproduced. Such quantities are, for instance, the collision energy, the quantum numbers defining the intramolecular state (vibrations and the principal quantum number of rotation), the total angular momentum etc. . . However, there are other dynamical variables which have a clear meaning in Classical Mechanics but correspond to no physical observable because of the Uncertainty Principle. We call them *phase variables* and denote them globally by g. The phase variables must be given particular values to obtain, at given G, a particular trajectory. Such variables are, for instance, the various intramolecular normal vibrational phases, the intermolecular orientation, the secondary rotation quantum numbers, the impact parameter, etc. . . Thus we look for relationships of the type $q_0 = q_0\,(G, g)$ and either $\dot{q}_0 = \dot{q}_0\,(G, g)$ or $p_0 = p_0\,(G, g)$

To reproduce the results of a given experiment whose theoretical specification is G we must obtain a set of trajectories for various g. Then the theoretical results (the energy transfer, the reaction probability, etc. . .) are obtained as averages over g. Thus an observable quantity F, observable at the end of the reaction, is calculated for given G as

$$F(G) = \sum_{i=1}^{N} F_i(G)/N$$

where:

$$F_i(G) = F(G, g_i) = F(q_0\,(G, g_i), \dot{q}_0\,(G, g_i)) \qquad (i = 1, 2 \ldots N).$$

N is the total number of trajectories. Here g_i is implicitly selected pseudo randomly[251, 252].

Sometimes an additional average over G is required to obtain the theoretical value of a macroscopic experimental quantity. Then one uses a normalized distribution function $P(G)$ of all the components of G, so that in application of the basic principles of Statistical Mechanics: $F = \int_\Gamma P(G)\, F(G)\, dG$ where Γ denotes the subspace of all the possible values of G under the given experimental conditions.

The integral is most often transformed into a finite sum. If the selected values G_j of G are regularly distributed over Γ, then:

$$F = \sum_{j=1}^{M} P(G_j)\, F(G_j) / \sum_{j=1}^{M} P(G_j)$$

where M is the total number of the G_j's. If they are selected pseudorandomly over Γ according to $P(G)$ as weighting function, then

$$F = \sum_{j=1}^{M} F(G_j)/M.$$

These expressions represent the most general theoretical results for whatever macroscopic experimental quantity F.

3. Unimolecular Reactions

In an unimolecular *thermal* reaction, *i.e.* a reaction whose mechanism is a pure intramolecular rearrangement (either isomerization or dissociation), the initial energy distribution among the various degrees of freedom of the system is unknown. Indeed, in a preliminary step the molecule acquires activation energy through a complex process (a collision or, rather, a sequence of collisions) which is in general badly elucidated experimentally. In addition the energy exchange between distortion modes of the activated molecule is very fast[14, 15].

Whenever the reaction involves a few atoms only, both the activation phase of the reaction and the subsequent unimolecular rearrangement can be studied dynamically[210–215]. Then it is possible to ascribe a statistical weight to a given trajectory. As soon as the reactant molecule includes numerous atoms (as is often the case in Organic Chemistry) one just cannot study the overall dynamics of the reaction. In particular, if one must renounce the investigation of the activation phase of the reaction, one must also renounce the attribution of statistical weights to individual trajectories. Then one must postulate, on the basis of either experimental information or physical intuition, initial activated states of the reactant system and study only its subsequent dynamical evolution. Thus the work is restricted to sample in a random way all the possible initial conditions with no attempt to obtain at the end theoretical values of experimental quantities. Nevertheless, this context is not too restrictive. The trajectory study of thermal unimolecular reactions allows one

(i) to discover which initial energy distributions favour completion of the reaction, which others disfavour or prevent it, and to relate these "a posteriori" observations to experimental facts;

(ii) to observe qualitatively the microscopic dynamical paths of the reactions;

(iii) to obtain the statistical distribution of the molecular lifetimes and thus to have a feeling for the reaction times at various total energies. Such a dynamical study of a unimolecular thermal reaction (isomerization of cyclopropane) is the subject of the next Chapter (C).

The situation just described is not inherent in all unimolecular reactions. In certain cases (for instance unimolecular *photochemical* reactions, *i.e.* non photosensitized) an equilibrium energetic distribution (that of the fundamental state in the case of photochemical reaction) is warranted. Then a statistical weight can be attributed to each trajectory, either classically or semi-quantally.

In the classical approach[253], the probability to find the ith normal coordinate of the system within $[q, q + dq]$ is proportional to the time elapsed in it:

$$P_i(E; q) = 2/\{T_i(E - k_i q^2/2)^{1/2}\}$$

where k_i and T_i are respectively the force constant and the period of the ith normal mode; E is the total energy in the mode (physical observable) and q is the phase variable. Thus the classical probability is minimal at equilibrium and infinite at the turning points of the vibration. Finally, the statistical weight of a set of initial conditions $\{G = E_1, E_2 \ldots; g = q_1, q_2 \ldots\}$ is the product of the partial probabilities for the various modes:

$$P(G; g) = \prod_{i=1,2\ldots} P_i(E_i; q_i)$$

In the semiquantal approach (theory of Wigner functions)[253–255], Statistical Mechanics is corrected according to quantum mechanical criteria. The statistical probability of finding the coordinate of the ith normal mode within $[q, q + dq]$ and its conjugate momentum within $[p, p + dp]$ is proportional to $\exp\{-[p^2/m_i + k_i q^2]/2\,kT\}$, where m_i and k_i and respectively the reduced mass and force constant of the ith mode, k is the Boltzmann constant and T is the temperature. There is no counterpart to this probability in Quantum Mechanics because of the Uncertainty Principle. However, since the normalized wave function $\Psi_i^v(p)$ of the ith normal mode in its vth vibrational state is known, the separate probabilities for q and p are entirely defined: $\Pi_i^v(q) = |\Psi_i^v(q)|^2$ and $\tilde{\Pi}_i^v(p) = |\Phi_i^v(p)|^2$ where $\Phi_i^v(p)$ is the Fourier transform of $\Psi_i^v(q)$. The meaning of these probabilities is the following: although it is impossible to predict the results of the simultaneous measurements of both q and p, it is nevertheless possible to predict the average results of measurements on a numerous set of identical systems if all of them are in the same quantum state. Thus it is quantum mechanically sound to look for a pseudo-distribution function $P_i(v; q, p)$ which would result in $\Pi_i^v(q)$ when integrated over p and in $\tilde{\Pi}_i^v(p)$ when integrated over q. Among all the mathematical functions fulfilling these two requirements, Wigner[254] has selected the very simple one:

$$P_i(v, q, p) = (\pi h)^{-1} \int_{-\infty}^{+\infty} \Psi_i^v(q + Q)\, \Psi_i^v(q - Q) \exp(2\,\mathrm{i}pQ/\hbar) dQ$$

$$= P_i(v; \xi_i^2) = (\pi h)^{-1} (-1)^v \exp(-\xi_i^2)\, L_v(2\,\xi_i^2)/(\pi\hbar v!)$$

where: $\xi_i^2 = \alpha_i^2 q^2 + p^2/(\alpha_i^2 h^2)$, α_i is a constant and L_v denotes a Laguerre polynomial. Here v is a physical observable and ξ^2 a phase variable. This function is real but not everywhere positive. For this reason it cannot be viewed as a true probability distribution function. Nevertheless, it can be used qua a distribution function since it fulfils all the requirements which would characterize this function if it existed. When $v = 0$, and only then,

$$P_i(v = 0; q, p) = \Pi_i^0(q) \times \tilde{\Pi}_i^0(p)$$

as it would be the case if p and q where simultaneously measurable[253]. When $v \neq 0$ the probability of a given p depends on q, and vice versa. In the classical limit (great values of v) this situation is consistent with the Correspondence Principle; indeed, in Classical Mechanics, the values of q and p are related to each other.

Finally, for a reactant system including several vibrational modes, the Wigner function is simply a product of one dimensional functions:

$$P(G = v_1, v_2 \ldots, g = \xi_1^2, \xi_2^2 \ldots) = \prod_{i=1,2\ldots} P_i(v_i, \xi_i^2)$$

One of us has personally applied the theory of Wigner functions to obtain statistical weights for individual trajectories in the study of the photochemical dissociation of the water molecule in its second singlet excited state[244, 256]:

$$H_2O(\tilde{B}\ ^1A_1) \longrightarrow H(^2S) + OH(^2\Sigma_+)$$

to account for the abnormally excited rotation of the OH fragment which is observed experimentally[257, 258].

C. Application: Optical and Geometrical Isomerizations of Cyclopropane

1. Experiments and Previous Theoretical Investigations

The pyrolysis of substituted cyclopropane leads to three types of unimolecular isomerizations (see Fig. 3). The first kinetic study of the conversion of cyclopropane into propylene (reaction a) was undertaken by Trautz and Winkler in 1922[l) 259]. The geometrical isomerization (reaction b) was discovered by Rabinovitch, Schlag, and Wiberg in 1958[m) 261]; reaction b is faster than structural isomerization in propylene (a). Finally, the optical isomerization was observed, independently by Crawford and Lynch[268], by Berson and Balquist[269], by Bergmann and Carter[270, 271], and by Willcott and Cargle[272]; their common conclusion states that geometrical (b) and optical (c) isomerizations are competitive reaction processes. If only the sub-

l) For a more recent experimental work on the mechanism of this reaction, see Ref.[260].

m) For later studies on *cis-trans* isomerization in substituted cyclopropanes, see Refs.[262–267].

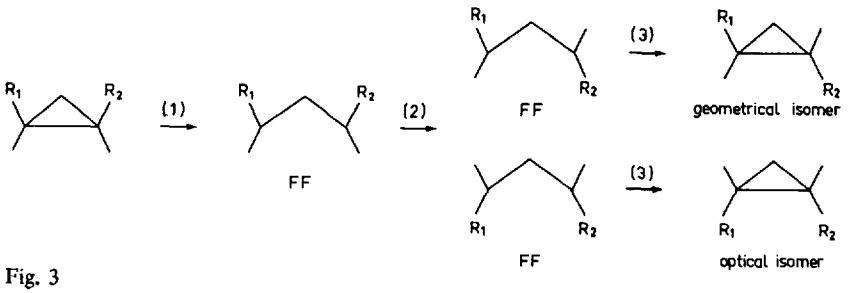

Fig. 3

stituted bond breaks, this result implies that the single-rotational process, required for geometrical isomerization, and the double-rotational process, required for optical isomerization, are competitive rotational processes. This was confirmed by Doering and Sachdev[273]. However, Berson, Pedersen and Carpenter have recently shown that in substituted cyclopropanes in which the three C–C bonds can break equally (*i.e.*: 1-phenylcyclopropane-2-d), the major pathway is a synchronous rotation of both terminal groups[274, 275]. Most mechanisms for the geometrical and optical isomerizations invoke a trimethylene diradical species (for a complete review, see Ref.[276]).

These reactions have aroused a great deal of interest among theoretical chemists. Indeed, they lie within the simplest reactions in organic chemistry; formally, they require only a rotation of 180° in one or both methylene groups. Hoffmann, in his

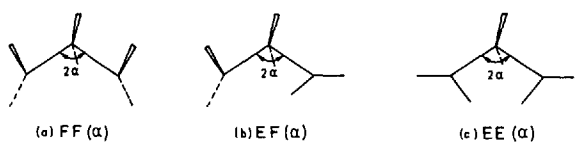

Fig. 4. Definition of the geometries of the three diradicals face-to-face [FF(α)], edge-to-face [EF(α)] and edge-to-edge [EE(α)]

pioneering search of the potential energy surface for isomerization of cyclopropane, found that synchronous (conrotatory) motion of the terminal groups, through an edge-to-edge (EE) diradical (Fig. 4-c) is the easiest path on the surface[277]. This prediction was recently confirmed by the kinetic analysis of the isomerization of trans-cyclopropane-1,2-d_2 by Berson and Pedersen[275]. Afterwards, several groups undertook nonempirical quantum-mechanical calculations on

(i) the ring opening of the cyclopropane and

(ii) the rotations of the terminal groups in the face-to-face (FF) diradical (Fig. 4-a) thus obtained[3, 4, 278–280]. The results of these calculations confirm the competition experimentally observed between the two isomerization reactions: the diradical EE is slightly more stable than the edge-to-face (EF, Fig. 4-b) diradical (ΔE = 1–2 kcal/mol). Moreover, no potential energy barrier is found in the ring closure of the diradical toward the cyclopropane. This result, inconsistent with thermodynamic pre-

dictions[281], is in agreement with the results of recent ESR study of 1,3-cyclopentadiyl diradical[282]. Finally, the geometry of the transition state for geometrical isomerization has been resolved in 21-dimensional space, and that for optical isomerization obtained approximately. Static reaction paths were proposed for both reactions b and c[3, 4].

II. Potential Energy Surface

The static study requires consideration of three main geometrical parameters: the angle of ring opening $\widehat{CCC}$ (= 2 α) and the rotation angles for both terminal methylene groups (θ_1 and θ_2). The other (secondary) parameters are either held constant or varied in a conventional way.

The potential energy function $V(\alpha, \theta_1, \theta_2)$ can be re-written as a sum of two terms:

$$V(\alpha, \theta_1, \theta_2) = V(\alpha, 0, 0) + [V(\alpha, \theta_1, \theta_2) - V(\alpha, 0, 0)] \tag{46}$$

The first term corresponds to the potential energy of a cyclopropane molecule in the FF configuration with the ring angle $\widehat{CCC}$ = 2 α (Fig. 4-a). The calculated energy curve is pictured in Fig. 5: there appears no barrier to the reclosure motion of the diradical FF (α). This curve will be analytically approximated by means of one-dimensional cubic spline functions.

The second term denotes the amount of energy required for rotations of the terminal groups, with angular amplitude of θ_1 and θ_2, at constant α. For each value of α, the potential energy of the diradical as a function of the two rotation angles is

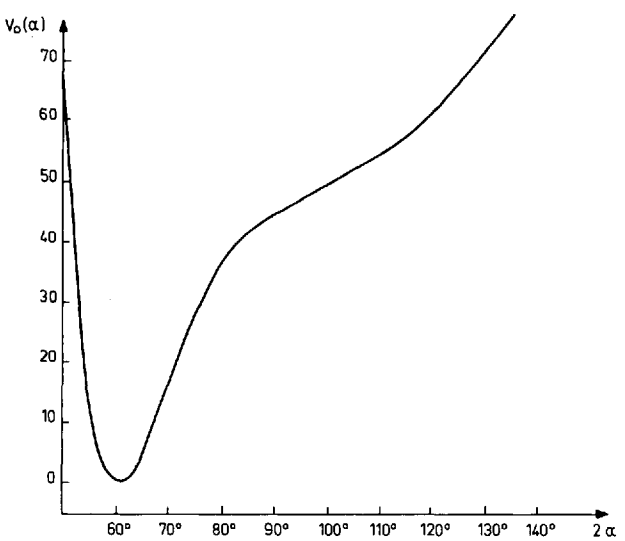

Fig. 5. Potential energy curve for the ring opening from cyclopropane to the face-to-face diradical. The energies are in kcal/mol

described by an analytical expression, which is simple but yet retains the essential features of the surface[1]. There are four main features of the rotational surfaces that the analytic formula must reproduce accurately: the energies of the half-way points EF(α) and EE(α); the potential-barrier heights, $h_C(\alpha)$ and $h_D(\alpha)$ for conrotatory and disrotatory motions (Fig. 6). The following analytic formula is somewhat arbitrary; it is selected because it abides by the law of symmetry and takes into account the four parameters independently:

$$\begin{aligned} V(\alpha,\theta_1,\theta_2) - V(\alpha,0,0) = {} & a(\alpha)\sin^2(\theta_1+\theta_2)\sin^2(\theta_1-\theta_2) \\ & + b(\alpha)\sin^2(\theta_1-\theta_2)\cos^2(\theta_1+\theta_2) \\ & + c(\alpha)\sin^2(\theta_1+\theta_2)\cos^2(\theta_1-\theta_2) \\ & + d(\alpha)\sin^2\theta_1\sin^2\theta_2 \end{aligned} \tag{47}$$

$a(\alpha)$ denotes the potential energy of the molecule in the configuration EF(α) ($\theta_1 = 90°$, $\theta_2 = 0°$) minus the potential energy of EF(α) ($\theta_1 = \theta_2 = 0°$). Similarly, $d(\alpha)$ is the potential energy of the molecule in the configuration EE(α) ($\theta_1 = \theta_2 = 90°$). $b(\alpha)$ and $c(\alpha)$ are simple functions of the potential energy barriers to the synchronous disrotatory motion [$h_D(\alpha)$] and the synchronous conratatory motion [$h_C(\alpha)$] respectively (see Fig. 6)

$$b(\alpha) = [h_D(\alpha) + (h_D^2(\alpha) - h_D(\alpha)\,d(\alpha))^{1/2}]/2 \tag{48}$$

$$c(\alpha) = [h_C(\alpha) + (h_C^2(\alpha) - h_C(\alpha)\,d(\alpha))^{1/2}]/2 \tag{49}$$

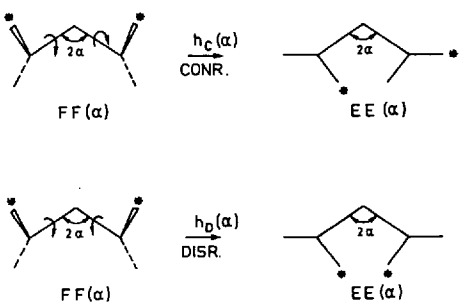

Fig. 6

Calculations of the energies were performed with a 3 x 3 CI version of Gaussian 70, at the STO-3G level[283]. For sixteen values of 2 α, regularly spaced form 50.1° = 0.875 rd to 136.1° = 2.375 rd, the potential energy curves which drive

(i) the synchronous conrotatory motion of both terminal methylene groups,

(ii) the synchronous disrotatory motion and

(iii) the rotation of a single methylene group (the other being held fixed) were computed. The computed values of $a(\alpha)$, $b(\alpha)$, $c(\alpha)$ and $d(\alpha)$ are interpolated by means of one-dimensional cubic spline functions.

The detailed results of these calculations have been given elsewhere[2]. Then we shall only recall the main features of the three-dimensional potential energy surface,

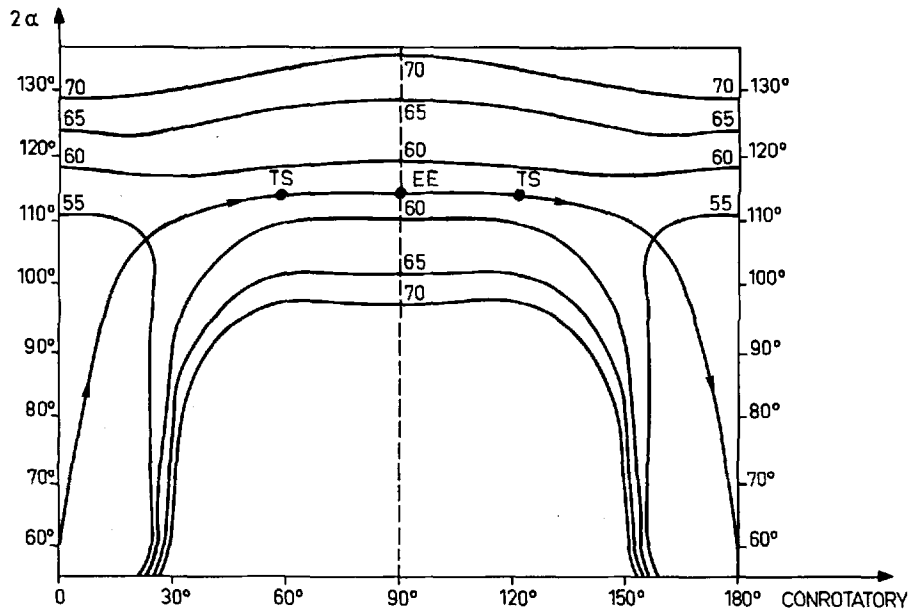

Fig. 7. Two-dimensional potential energy surface and static reaction path for the synchronous conrotatory motion of the terminal methylene groups. 2α represents the value of the carbon ring angle. The abcissa gives the common value of both rotational angles: $\theta = \theta_1 = \theta_2$. TS denotes the position of a transition state. The energies are in kcal/mol

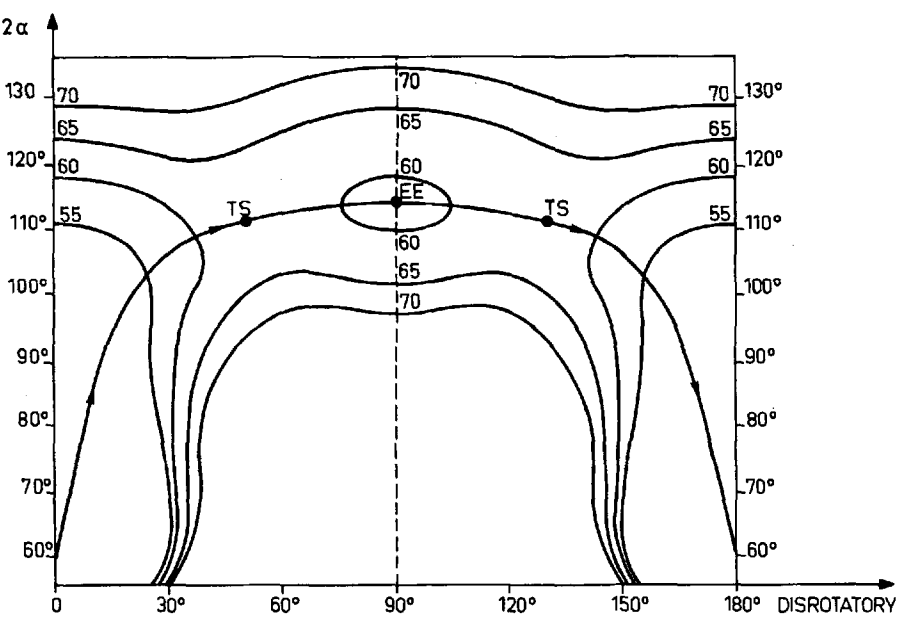

Fig. 8. Two-dimensional potential energy surface and static reaction path for the synchronous disrotatory motion of the terminal methylene groups. 2α represents the value of the carbon ring angle. The abcissa gives the common absolute value of both rotational angles: $\theta = \theta_1 = -\theta_2$. TS denotes the position of a transition state. The energies are in kcal/mol

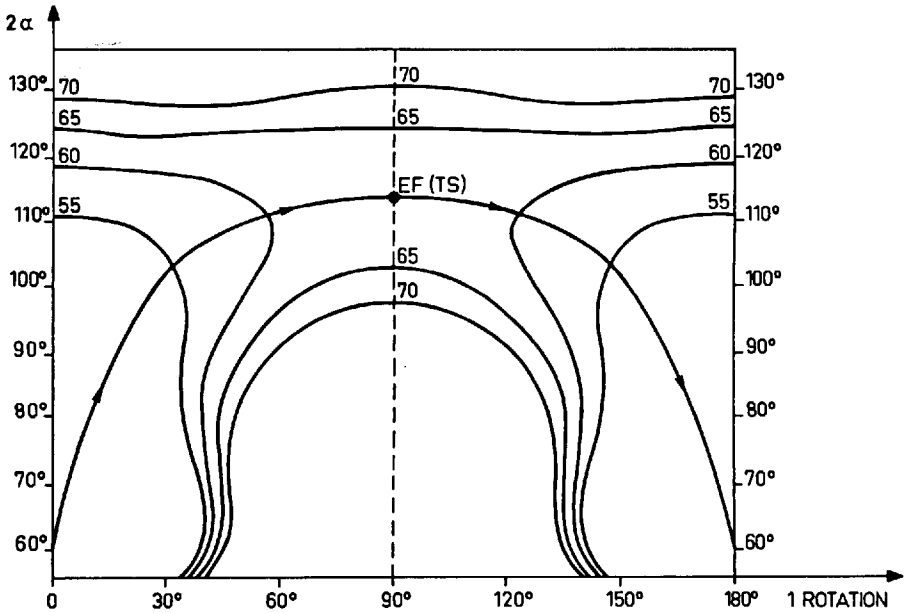

Fig. 9. Two-dimensional potential energy surface and static reaction path for the rotational motion of a single terminal methylene group. 2α represents the value of the carbon ring angle. The abcissa gives the value of the rotational angle: $\theta = \theta_1$ along with $\theta_2 = 0$. TS denotes the position of a transition state. The energies are in kcal/mol

by means of two-dimensional cuts obtained in the following three limiting cases:

(i) synchronous conrotatory motion ($\theta_1 = \theta_2 = \theta$; cf. Fig. 7);

(ii) synchronous disrotatory motion ($\theta_1 = -\theta_2 = \theta$; cf. Fig. 8);

(iii) rotation of a single methylene group ($\theta_1 = 0$, $\theta_2 = \theta$; cf. Fig. 9). The minimum energy paths are drawn approximately and the positions of the transition states (TS) are specified.

The main features of the overall surface appears clearly in these two-dimensional cuts: in a first step, the reaction coordinate is almost identical with a pure ring-opening motion; the rotation of the terminal groups occurs at almost constant angle $\widehat{CCC}$, and finally the ring recloses and the isomer molecule is formed. The optical isomer is most easily formed via a purely conrotatory process (see Fig. 7). The transition state is close to EE (α) with $2\alpha = 113°$ and is energetically located at 59.8 kcal/mol above cyclopropane. In Fig. 8, the diradical EE (α) with $2\alpha = 113°$ appears to be a secondary minimum along the synchronous disrotatory reaction path. In fact, it is not a true minimum, since a conrotatory distortion (here, the hidden third coordinate) requires practically no activation energy. The optical isomerization via a synchronous disrotatory process requires an activation energy of 61.9 kcal/mol. At last, the transition state for geometrical isomerization (cf. Fig. 9) is the diradical EF (α) with $2\alpha = 113°$ whose potential energy is 61.6 kcal/mol above that of cyclopropane.

III. Dynamical Study

1. Equations of Motion and Initial Conditions

The equations of motion are established within the following simplification: the kinetic energy of the system is written for a model in which the terminal methylene groups remain trigonal throughout the reaction (see Fig. 10). Then, the $\underset{\sim}{A}$ matrix, defined in a previous section, is diagonal and the expression of the kinetic energy is a diagonal quadratic form of the angular velocities:

$$T = \frac{1}{2} A_{\alpha\alpha} \dot{\alpha}^2 + \frac{1}{2} I (\dot{\theta}_1^2 + \dot{\theta}_2^2) \tag{50}$$

where: $A_{\alpha\alpha} = S \sin^2\alpha + C \cos^2\alpha + I(\sin^2\theta_1 + \sin^2\theta_2)$ (51)

and: $$S = \frac{2}{M + 2m_1} \left\{ \frac{1}{1 + 2\rho} [L(M + 2m_1) + 2m_1\lambda]^2 + M 2m_1\lambda^2 \right\}$$

$$C = 2[ML^2 + 2m_1(L + \lambda)^2]$$

$$I = 2m_1\mu^2$$

$$\rho = \frac{M + 2m_1}{M + 2m_2}$$

$$\lambda = l\cos\frac{\gamma}{2}, \quad \mu = l\sin\frac{\gamma}{2}$$

L is the CC length, l the CH length and γ the $\hat{HCH}$ angle in the terminal groups, M the mass of a carbon atom, m_1 and m_2 the masses of the substituents on $C_1(C_2)$ and C_3 respectively. In the present study $m_1 = m_2 = 1$ and $\rho = 1$; I is the moment of inertia of the rotor which is formed of the two hydrogen atoms in a terminal methylene group. Eq. (51) leads to the partial derivatives:

$$\frac{\partial A_{\alpha\alpha}}{\partial\alpha} = (S - C)\sin 2\alpha \tag{52}$$

$$\frac{\partial A_{\alpha\alpha}}{\partial\theta_i} = I\sin(2\theta_i) \qquad (i = 1, 2) \tag{53}$$

Finally, the three Lagrangian equations of motion are:

$$\ddot{\alpha} = -\frac{1}{A_{\alpha\alpha}} \left[\frac{1}{2} \frac{\partial A_{\alpha\alpha}}{\partial\alpha} \dot{\alpha}^2 + \dot{\alpha} \left(\frac{\partial A_{\alpha\alpha}}{\partial\theta_1} \dot{\theta}_1 + \frac{\partial A_{\alpha\alpha}}{\partial\theta_2} \dot{\theta}_2 \right) + \frac{\partial V}{\partial\alpha} \right] \tag{54}$$

$$\ddot{\theta}_i = \frac{1}{I} \left[\frac{1}{2} \frac{\partial A_{\alpha\alpha}}{\partial\theta_i} \dot{\alpha}^2 - \frac{\partial V}{\partial\theta_i} \right] \qquad (i = 1, 2) \tag{55}$$

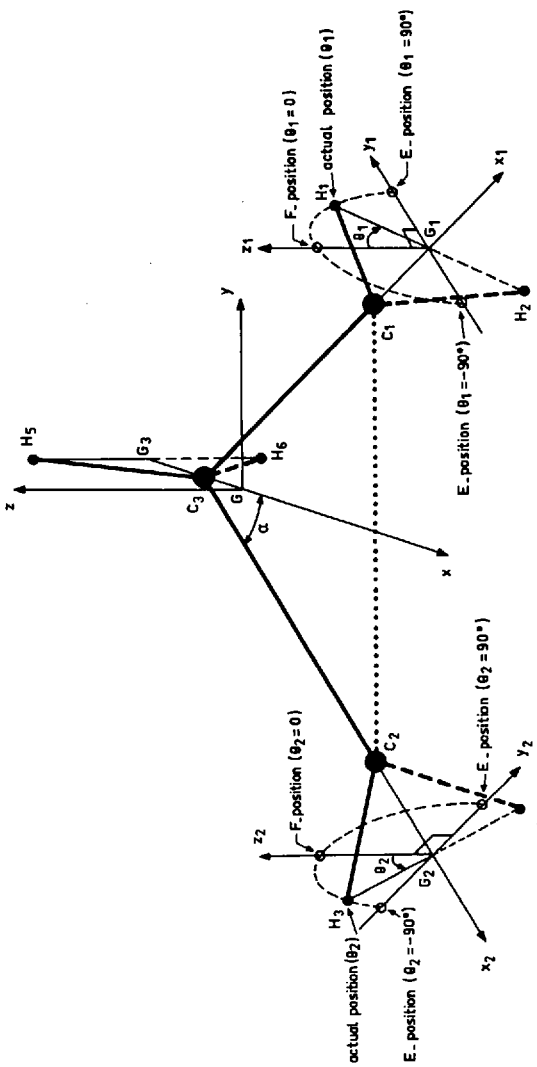

Fig. 10. Definition of the dynamical variables α, θ_1 and θ_2. Particular molecular conformations are explicitly indicated

where:

$$\frac{\partial V}{\partial \alpha} = \frac{dV_0}{d\alpha} + \frac{da}{d\alpha}\sin^2(\theta_1+\theta_2)\sin^2(\theta_1-\theta_2) + \frac{db}{d\alpha}\sin^2(\theta_1-\theta_2)\cos^2(\theta_1+\theta_2)$$
$$+ \frac{dc}{d\alpha}\sin^2(\theta_1+\theta_2)\cos^2(\theta_1-\theta_2) + \frac{dd}{d\alpha}\sin^2\theta_1\sin^2\theta_2 \qquad (56)$$

$$\frac{\partial V}{\partial \theta_i} = 2\sin(2\theta_i)\ \pm a(\alpha)\sin(\theta_1+\theta_2)\sin(\theta_1-\theta_2) \pm b(\alpha)\sin(\theta_1-\theta_2)\cos(\theta_1+\theta_2)$$
$$+ c(\alpha)\sin(\theta_1+\theta_2)\cos(\theta_1-\theta_2) + \frac{1}{2}d(\alpha)\sin^2\theta_{i'}$$
$$(i = 1, 2 \text{ and } i' \neq i) \qquad (57)$$

The + alternative should be used for $i = 1$ and the − alternative for $i = 2$ respectively.

The numerical integration of the three coupled second order differential Eq. (54), (55) requires six initial conditions. These are (i, ii, iii) the three values $2\alpha^\circ$, θ_1° and θ_2°, which determine the molecular geometry at the starting point (all the trajectories in the present study start with the cyclopropane molecule in its equilibrium geometry, *i.e.* $2\alpha^\circ = 60^\circ$, $\theta_1^\circ = \theta_2^\circ = 0$); (iv) the total internal energy in the molecule, E_{tot}; (v) the fraction E_{rot}° of initial energy attributed to the "rotation" (at starting point, this is actually vibration energy); (vi) the manner in which E_{rot}° is distributed among the two "rotors". This is defined by an angle (δ°) such that:

$$\mathrm{tg}\delta^\circ = \dot{\theta}_1^\circ/\dot{\theta}_2^\circ \qquad (58)$$

where $\dot{\theta}_1^\circ$ and $\dot{\theta}_2^\circ$ are the initial rotational velocities of the two groups. Then the relationship:

$$\dot{\theta}_2^\circ = \cos\delta^\circ\,[2I^{-1}E_{rot}^\circ]^{1/2} \qquad (59)$$

is used. It is not restrictive to have $\dot{\theta}_2^\circ > 0$ since $\dot{\theta}_1^\circ$ can be either positive or negative. A third relationship:

$$\dot{\alpha}^\circ = \pm\{2\,[E_{tot} - E_{rot}^\circ - V(\alpha^\circ, \theta_1^\circ, \theta_2^\circ)]/A_{\alpha\alpha}(\alpha^\circ, \theta_1^\circ, \theta_2^\circ)\}^{1/2}, \qquad (60)$$

is necessary to define the initial $\widehat{CCC}$ angular velocity. The present study has been arbitrarily limited to $\dot{\alpha}^\circ > 0$, *i.e.* to initial extensions of the CC bond.

Five different values of E_{tot} have been studied, namely 61, 62, 63, 64 and 65 kcal/mol. For $E_{tot} = 61$ kcal/mol, the only available channel is the synchronous conrotatory motion (transition state at 59.8 kcal/mol). For $E_{tot} \geqslant 62$ kcal/mol, the rotation of a single group (transition state at 61.6 kcal/mol) and the concerted disrotatory motion (transition state at 61.9 kcal/mol) both become feasible motions, at least in principle. For each value of E_{tot}, E_{rot}° has been varied stepwise from 2 to 50 kcal/mol, with a step of 2 kcal/mol. In addition, for given values of E_{tot} and E_{rot}°, δ° has been varied from 45° (conrotatory motion, *i.e.* antisymmetric vibra-

tion of the methylene groups) to −45° (disrotatory motion, *i.e.* symmetric vibration), with a step of 10°. All things considered, about 1500 trajectories have been run.

In our model, no fraction of the total energy in the molecule can be transferred to nonreactive intramolecular modes; nor can any fraction be exchanged with the medium. Under this assumption the computed trajectories are endless: a given set of initial conditions leads to an infinite sequence of ring openings, rotations and ring closures. The integration of a trajectory is stopped the first time the representative point of the molecule moving on the surface enters a prescribed narrow region around the absolute minimum, *i.e.* the representative point of cyclopropane in its equilibrium geometry. This is consistent with the analysis of the reaction given by Doering and Sachdev[273] within the RRK-model[13]. Their conclusion was that "the best trap for a diradical is its own reclosure to a covalent bond", because there the energy "is rapidly dissipated by distribution among other, non-reactive modes. The larger the number of atoms . . . in the molecule, the more nearly true this statement is".

2. Dynamical Results

We first treat separately the trajectories corresponding to the particular values $\delta° = 45°$ and $-45°$. Indeed, the total symmetry of the problem is such that, whenever the motion of both rotors at the starting point is either purely conrotatory or purely disrotatory, it keeps this particularity throughout the trajectory. Then the trajectory can be drawn on a two-dimensional potential energy surface such as that pictured in Fig. 7 and 8.

a) Synchronous Conrotatory Motion ($\delta° = 45°$). For a very weak amount of excess energy (1.2 kcal/mol) with respect to the conrotatory transition state (59.8 kcal/mol), a rather striking phenomenon occurs: reactive trajectories are observed

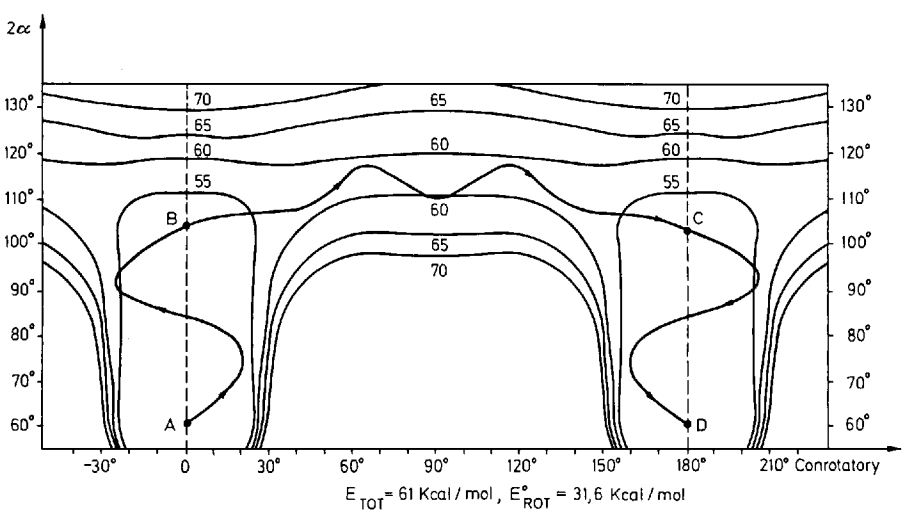

Fig. 11. A low total energy (61 kcal/mol) reactive trajectory leading from cyclopropane to the optical isomer via a purely conrotatory process ($\delta° = 45°$)

only when E°_{rot} – initial "rotational" energy here exclusively in the antisymmetric twisting vibration of the methylene groups – lies between 30.4 and 32.4 kcal/mol (see Fig. 11). Thus, in order to observe the optical isomer formed in a purely conrotatory fashion, one half of the total molecular internal energy must be placed in the methylene groups. The other half of the total energy (28.6 to 30.6 kcal/mol) remains in the stretching vibrational mode of the carbon-carbon bond. At first sight, this would seem insufficient to bring about the opening of the carbon ring. However, during the first part of the reaction (from point A to point B in Fig. 11), the ring opening motion and a complete oscillation of both terminal groups (with an amplitude of 20°) go on simultaneously. Hence, an important energy transfer occurs from the methylene groups to the carbon-carbon bond. Then only, the carbon ring can open. Afterwards, the methylene groups rotate by 180° (from B to C in Fig. 11); in the meantime the value of the $\hat{CCC}$ angle oscillates weakly around the optimum value 113°. The reaction ends with a motion of ring closure (from C to D in Fig. 11).

When the total intramolecular energy increases ($E_{tot} \geqslant 62$ kcal/mol), the reactive trajectories are more numerous. Below we analyze in detail the set of trajectories for $E_{tot} = 62$ kcal/mol (see Fig. 12). Depending on the value of E°_{rot}, several distinguishable motions are observed:

$E^{\circ}_{rot} \leqslant 10$ kcal/mol: the trajectories are non reactive. As shown in Fig. 12a, the carbon ring opens and recloses without reaching the transition state. This is simply due to a lack of twisting energy in the methylene groups at the starting point.

$12 \text{ kcal/mol} \leqslant E^{\circ}_{rot} \leqslant 20$ kcal/mol: within these limits the trajectories are reactive (see Fig. 12b, c and d). They are quite different from the trajectories in Fig. 11: only one half of an oscillation of the methylene groups occurs during the ring-opening phase. In Fig. 12b the first reactive trajectory of this type is pictured: during the rotation of the methylene groups the carbon ring angle oscillates many times around the optimum value 113° and, consequently, the duration of the phase of rotation is long (3.3×10^{-13} second). This means, that the way in which the representative point reaches the upper valley is far from being ideal. The ideal situation occurs when $E^{\circ}_{rot} = 16$ kcal/mol (see Fig. 12c); then, the methylene groups rotate very easily in 2.2×10^{-13} second. Finally, for $E^{\circ}_{rot} = 20$ kcal/mol (see Fig. 12d) the rotational process is again difficult and lengthy (4.4×10^{-13} second). It is quite important to note that all these trajectories include only a *single rotation of 180°* by each terminal group. This result is all the more surprising since the energy in the rotational motion can only be transferred, in our model, to the vibration of the carbon-carbon bond, and not to a non reactive mode.

$22 \text{ kcal/mol} \leqslant E^{\circ}_{rot} \leqslant 32$ kcal/mol: the trajectories are non-reactive, as pictured in Fig. 12e and 12f. When the ring opens the energy is badly distributed among the different possible modes and the transition state cannot be reached. In Fig. 12e, the representative point, after a half oscillation of the methylene groups, bounces off the edge of the lower potential energy bump towards the upper part of the figure. In Fig. 12f, the same thing occurs, but after a complete oscillation.

$32.4 \text{ kcal/mol} \leqslant E^{\circ}_{rot} \leqslant 35.2$ kcal/mol: within these limits the trajectories are again reactive (see Fig. 12g) and of the same type as that pictured in Fig. 11. As previously, each terminal group rotates by only 180°. It should be emphasized that this second "reactive band" of initial rotational energies is much more narrow than the

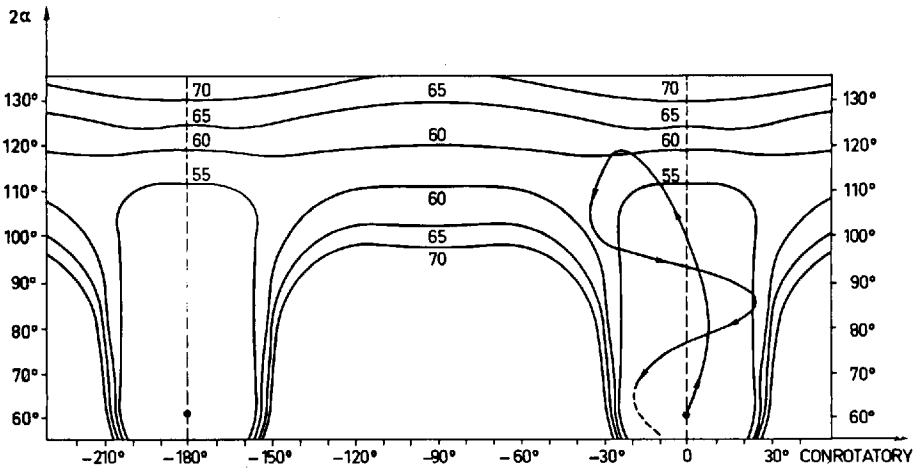

(a) E°_{ROT} = 6 Kcal/mol

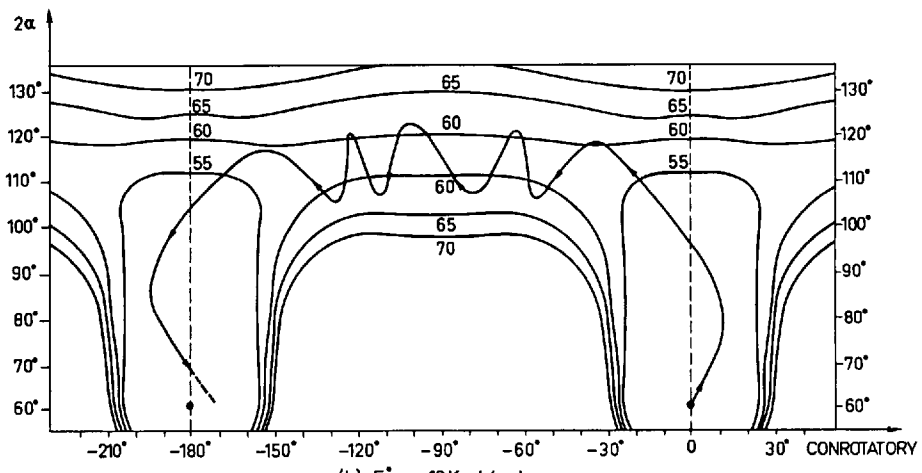

(b) E°_{ROT} =12 Kcal/mol

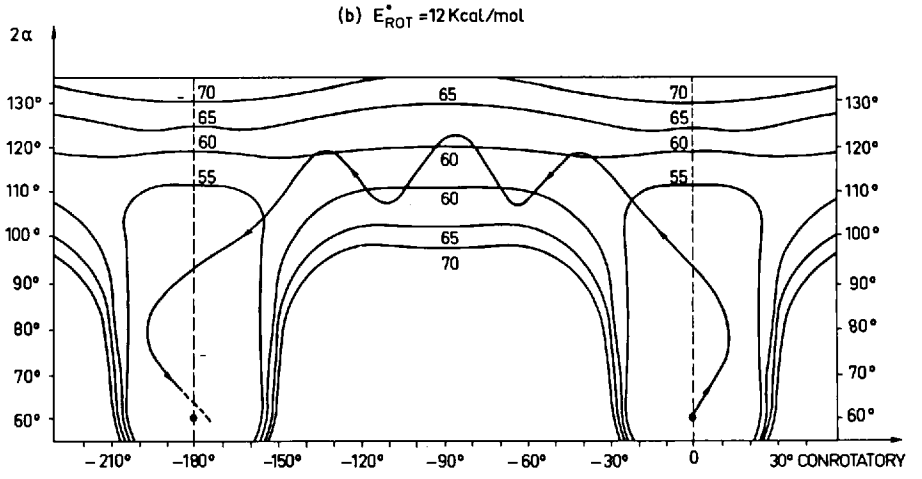

(c) E°_{ROT} = 16 Kcal / mol

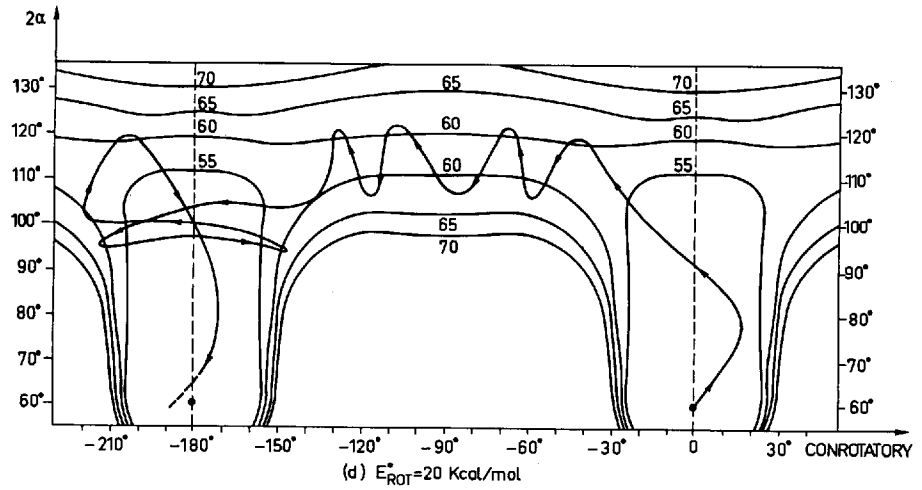

(d) E°_{ROT}=20 Kcal/mol

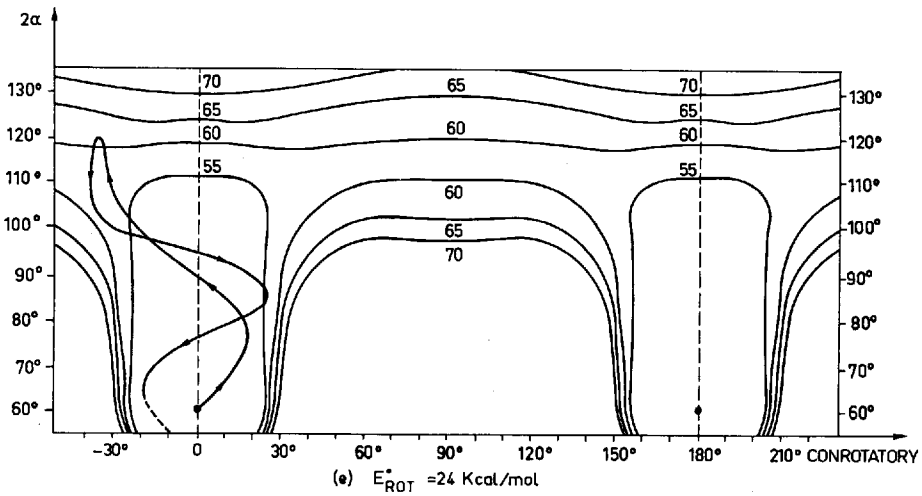

(e) E°_{ROT} =24 Kcal/mol

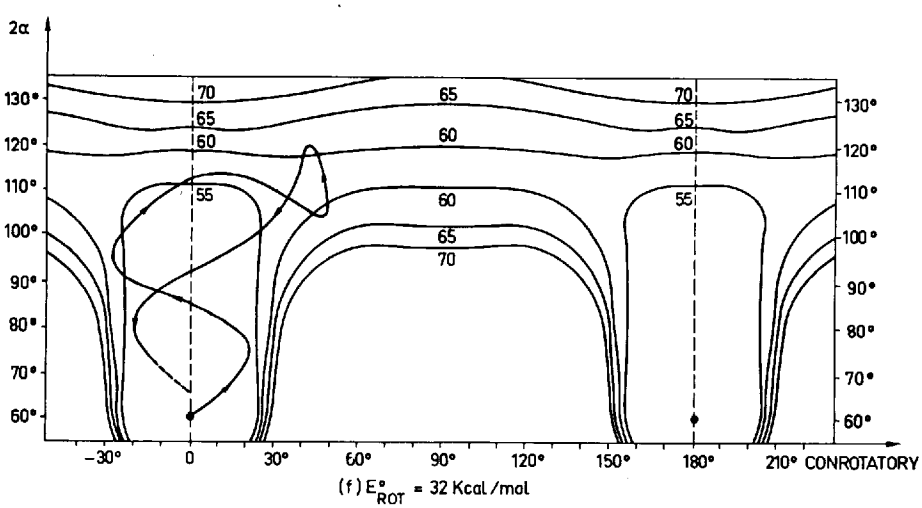

(f) E°_{ROT} = 32 Kcal/mol

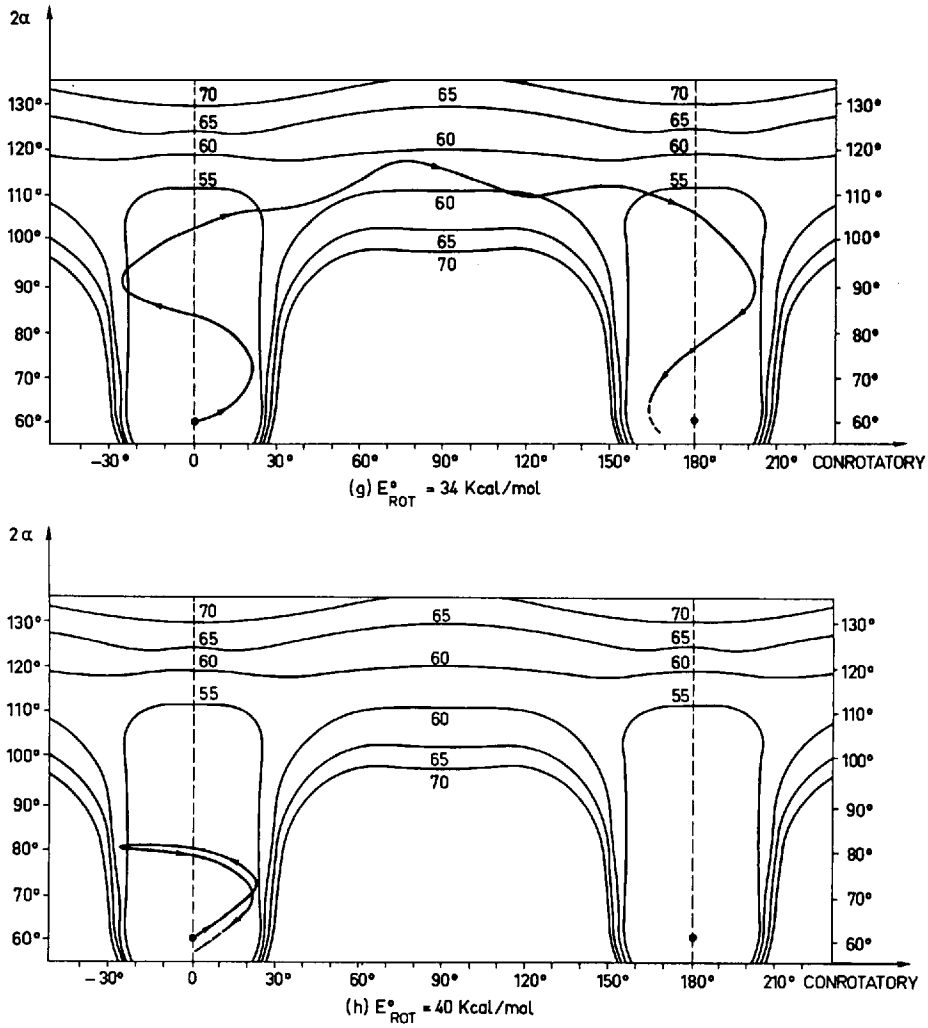

Fig. 12. Typical conrotatory trajectories at E_{tot} = 62 kcal/mol for different initial "rotational" (vibrational) energies

first one. This can be explained as follows: the rotations occur after a complete oscillation of the methylene groups. As a consequence, this first part of the reaction (ring opening) lasts longer in the trajectories of the second band (32.4 to 35.2 kcal/mol) than in the trajectories of the first "reactive band" (12 to 20 kcal/mol). Then the reactive trajectories are much more "focused" around the ideal trajectory: a slight modification can lead to large deviations and rapidly to non reactive trajectories.

$E^{\circ}_{rot} \geqslant 36$ *kcal/mol:* these trajectories are non reactive (see Fig. 12h). The energy initially concentrated in the stretching mode of the carbon-carbon bond is too small ($\leqslant$ 26 kcal/mol) to allow a sufficient opening of the carbon ring.

For total intramolecular energies greater than 62 kcal/mol, (E°_{tot} = 63, 64, 65 kcal/mol), the two "reactive bands" of initial E°_{rot} values still exist (see Fig. 13a) and even become larger and larger with increasing E_{tot}[n) 285)]. This is due to the fact that, the greater the excess energy, the easier it is for the representative point of the molecule to step over the transition state, even if the approach coordinate is not favourable. Moreover, the second reactive band shifts slightly towards higher values of E°_{rot}, so that the first phase of the reaction (ring opening along with a complete oscillation of the methylene groups) always results in a face-to-face diradical with a $\widehat{CCC}$ angle close to 105°.

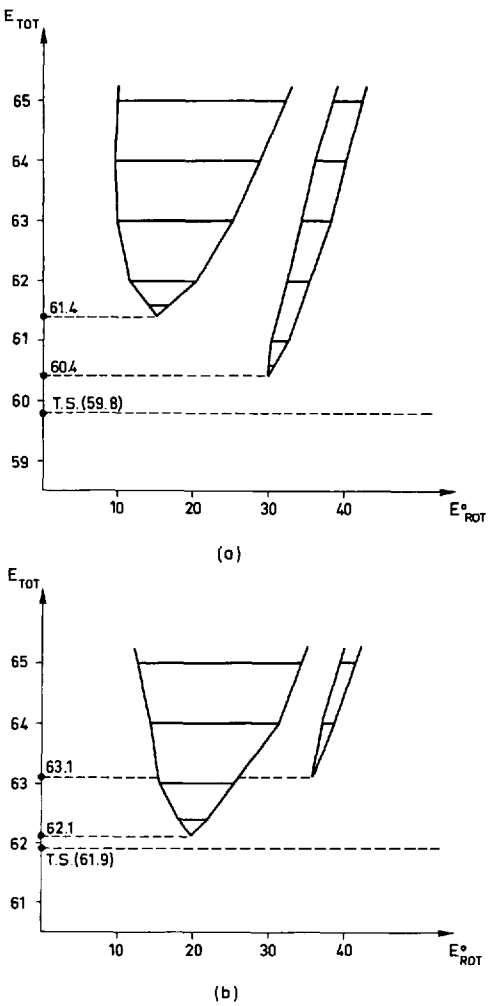

Fig. 13. Evolution of the "reactive bands" versus E_{tot} and E°_{rot} for (a) a conrotatory motion of the terminal groups and (b) a disrotatory motion

n) A long time ago, Wall and Porter[90)] have mentioned the existence of upper energy bounds for H + H_2 collinear reactions. More recently, Wright *et al.*[284)] have observed quite similar reactive and unreactive "bands" for exchange reactions resulting from collinear atom-molecule collisions.

The results presented in this section all depend strongly on the assumption which allowed us to terminate the trajectories. For instance, certain "reactive" trajectories, if they were free to go on, could come back to the starting point of the reaction. Conversely, certain "non-reactive" trajectories, after the first process of ring opening and closure, could yield a cyclopropane molecule possessing a more suitable amount of CH_2 vibration energy and the isomerization reaction could now be possible (Fig. 12a). Furthermore, the treatment of the dynamical problem in its *full dimensionality* might well make the unreactive region between the two reactive bands disappear.

b) Synchronous Disrotatory Motion ($\delta° = -45°$). The main results of the previous section for conrotatory trajectories remain true in the case of disrotatory trajectories. According to the value of E°_{rot} (here the initial CH_2 symmetric vibration energy), two reactive bands are still observed and exhibit the same characteristics as above; the first band corresponds to values of E°_{rot} of the order of 20 kcal/mol and the second band to values of E°_{rot} of the order of 40 kcal/mol. Most of the reactive trajectories involve a single concerted rotation of the terminal groups.

The only noticeable difference concerns the nature of the reactive trajectories when the total energy is only weakly in excess of that of the transition state. For the lowest total intramolecular energy studied (E_{tot} = 63 kcal/mol, *i.e.* $E_{tot} - E_{T.S.}$ = 1.1 kcal/mol), we observed reactive trajectories in the first band only, *i.e.* for E°_{rot} lying between 16 and 26 kcal/mol. This is exactly opposite to what happens in the case of a synchronous conrotatory motion at E_{tot} = 61 kcal/mol ($E_{tot} - E_{T.S.}$ = 1.2 kcal/mol) where reactive trajectories are observed in the second band only. The difference is probably due to the disrotatory transition state lying closer to the entrance valley than the conrotatory transition state (the top of the rotational barrier is at $\theta_1 = -\theta_2 = 50°$ presently, instead of $\theta_1 = \theta_2 = 58°$ before). Moreover, the entrance valley which drives the ring opening is wider in the disrotatory case than in the conrotatory case because disrotatory distortions require a smaller amount of energy than conrotatory distortion, as long as $2\alpha < 95°$.

More precise calculations indicate that the first reactive band appears at E_{tot} = 62.1 kcal/mol and the second reactive band at E_{tot} = 63.1 kcal/mol. The evolution of the reactive band widths versus the total energy is represented in Fig. 13b.

The small secondary minimum (well depth: 2.3 kcal/mol) at the edge-to-edge half-way point does not affect the trajectories very much even for the lowest total energy. However, there are some rare exceptions where the representative point of the molecule spends rather a long time in this region of the potential energy surface (for certain trajectories, the integration was stopped after $1.5\ 10^{-12}$ second and the molecule was still trapped into the well). Then, the final outcome of the reaction is quite a random phenomenon.

c) General Motion (General $\delta°$). When $\delta°$ differs from $\pm 45°$, the coupling between the rotations of both methylene groups results, at anytime, in an energy transfer from one to the other. Then the first question arises: for a given value of $\delta°$ characterizing the distribution of the initial methylene "rotation" (vibration) energy, what is the actual value of $\delta = \mathrm{tg}^{-1}(\dot{\theta}_1/\dot{\theta}_2)$ after the ring-opening phase of the reaction is terminated?

Table 3. Nature of the half-way point for reactive trajectories, depending on the values of $\delta°$ and $E°_{rot}$, when E_{tot} = 62 kcal/mole. The blank terms of the array correspond to non reactive trajectories

$\delta°$	$E°_{rot}$																								
	2	4	6	8	10	12	14	16	18	20	22	24	26	28	30	32	34	36	38	40	42	44	46	48	50
−45°																									
−35°																									
−25°																									
−15°																									
−5°																									
5°																									
15°																									
25°							EE_C	EE_C	EE_C								EE_C								
35°						EE_C	EE_C	EE_C	EE_C	EE_C		EE_C					EE_C								
45°						EE_C	EE_C	EE_C	EE_C	EE_C							EE_C								

Table 4. Nature of the half-way point, depending on the values of δ° and E°_{rot}, when E_{tot} = 63 kcal/mole. The blank terms of the array correspond to non reactive trajectories. Several rotations within the diradical lead either to the starting molecule (1) or to the geometrical isomer (2)

δ°	E°_{rot}																							
	2	4	6	8	10	12	14	16	18	20	22	24	26	28	30	32	34	36	38	40	42	44	46	48	50
−45°								EE_D	EE_D	EE_D	EE_D	EE_D	EE_D												
−35°								EE_D	EE_D	EE_D	EE_D	EE_D	EE_D												
−25°								EF	EF	$EF^{(1)}$	$EE_D^{(1)}$	EE_D	EE_D				EF	EF							
−15°								EF	EF	EF	EF	EF	EE_D					$EF^{(2)}$							
−5°								$EF^{(2)}$	EF	EF	EF	EF						EE_D	$EF^{(2)}$						
5°								EE_C	EE_C	EF	EF							EF	EE_D						
15°							$EE_C^{(1)}$	EE_C	EE_C	EE_C	EE_C							EF	EF						
25°						EE_C	EE_C	EE_C	EE_C	EE_C	EE_C							EE_C							
35°						EE_C	EE_C		EE_C		EE_C	EE_C	EE_C					EE_C							
45°					EE_C	EE_C	EE_C		EE_C	EE_C		EE_C						EE_C	EE_C						

In Ref.[1], we noted that the process of ring-opening is much faster than the rotations of the terminal groups whatever the type of cyclopropane molecules, either substituted or not. Consequently, energy transfer between the two oscillating terminal groups does not have time to operate significantly while the carbon ring opens. The opened molecule is rather similar to a FF-type diracial whose CH_2 rotational energy – which is possibly very different from E°_{rot} – is nevertheless distributed among both rotors in almost the same way as that defined by δ° at starting point. A careful study of the relative variations with time of θ_1 and θ_2 leads to the following conclusion. Whatever, the value of δ°, the corresponding trajectory, when reactive, closely resembles the reactive trajectory obtained for the same value of δ° on the rotational potential energy surface at constant $\widehat{CCC}$ angle (see Ref.[1], Fig. 7). Thus, if $\delta^{\circ} > 0$, the rotation of the terminal groups most frequently leads, *via* a conrotatory process, to a molecular conformation close to that of an edge-to-edge diradical (EE_C). If $\delta^{\circ} < 0$, we observe either the rotation of a single terminal group (EF), or within a narrow range close to -45°, the formation via a disrotatory process of an edge-to-edge diradical (EE_D). It should be emphasized that, whatever the value of δ°, both reactive bands (corresponding to values of E°_{rot} of the order of 20 and 40 kcal/mol respectively) are still observed. At low total energy (62 kcal/mol), all the reactive trajectories lead to the formation of the diradical EE_C via a *synchronous* conrotatory motion of both terminal methylene groups (cf. Table 3). The amount of excess energy above the potential energy of the transition state is weak (2.2 kcal/mol), so that it is only within the range $\delta^{\circ} \geqslant 25^{\circ}$ that the reaction is possible. The ring reclosure occurs after only a single concerted 180° rotation of the terminal groups. For $E_{tot} \geqslant 63$ kcal/mol, the three distinct rotational processes within the diradical species are now possible (cf. Table 4). When δ° varies from 45° to -45°, we observe successively the concerted conrotatory process, the rotation of a single group and, last, the concerted disrotatory process. Reactive trajectories involving several rotations in the diradical appear. They correspond, most frequently, either to limits (on the reactive side) between "reactive" and "non reactive" bands, or within a reactive band, to limiting values of δ° and E°_{rot} beyond which there is a change in the nature of the isomer formed.

3. Conclusion

The dynamical study of the coupling between the modes of ring opening (and closure) and the modes of rotation of the methylene groups of a cyclopropane molecule in the course of isomerization reactions confirms essentially the two main conclusions of the static study:

(i) an isomerization involves, at least approximately, three sequential steps: ring opening, methylene rotation(s) and ring closure;

(ii) the concerted conrotatory motion of the terminal groups is the easiest reaction path.

This study also brings new information which could not be derived from the only study of the potential surface:

(i) the amount of methylene "rotation" (vibration) energy required for the reaction to be possible is much larger than was previously estimated;

(ii) in general, a single rotation of 180° of one or both terminal groups occurs within the diradical species.

General Conclusion

The dynamical study of mechanistic details in organic reactions is complementary to the static study of the potential energy surface. It furnishes a supplement of information which cannot be obtained from the static surface alone.

The question which must be raised now is: "Is this type of study called for and will it be of common use in the future?" A first limitation is of a technical nature: the dynamical study may be of interest only when the potential energy surface driving the reaction is known with sufficient accuracy. Thus the range of application is restricted to reaction systems involving rather simple molecules. A second limitation is that such a dynamical study is almost necessarily incomplete; for instance, in most cases this precludes the obtaining of the reaction rates of organic reactions.

The purpose of such dynamical studies is mainly the development of a dynamical intuition among chemists. Once the potential energy surface of reaction is known, this intuition could allow qualitative predictions of

(i) possible deviations of the actual trajectories compared to the static minimum energy path;

(ii) those energy distributions in reagents which favour completion of the reaction, etc. . .

In this respect, dynamical studies of a limited number of typical reactions are highly desirable. The rapid improvement of both the means of calculation and the experimental techniques which result in having access to more and more tiny details of reaction mechanisms, should stimulate research work in this direction.

Acknowledgements. We gratefully acknowledge the assistance of Professor L. Salem who introduced us to the dynamical study of the isomerization of cyclopropane, Professor J. M. Lehn who suggested to us to write the present article, Dr. G. Bergeron who read the manuscript, Professor F. Fiquet-Fayard, Dr. M. Sizun and Dr. S. Goursaud who made available to us part of their work and Dr. F. Flouquet for helpful discussions.

References

[1] Jean, Y., Chapuisat, X.: J. Amer. Chem. Soc. *96*, 6911 (1974).
[2] Chapuisat, X., Jean, Y.: J. Amer. Chem. Soc. *97*, 6325 (1975).
[3] Jean, Y., Salem, L., Wright, J. S., Horsley, J. A., Moser, C., Stevens, R. M.: Pure Appl. Chem., Suppl. *1*, 197 (1971).
[4] Horsley, J. A., Jean, Y., Moser, C., Salem, L., Stevens, R. M., Wright, J. S.: J. Amer. Chem. Soc. *94*, 279 (1972).
[5] Jean, Y., Thesis: Isomerisation géométrique du cyclopropane. Orsay 1973.
[6] Chapuisat, X., Thesis: Etude dynamique des réactions chimiques: isomerisations optique et géométrique du cyclopropane. Orsay 1975.
[7] Bunker, D. L.: Meth. Comp. Phys. *10*, 287 (1971) and references therein.
[8] Secrest, D.: Ann. Rev. Phys. Chem. *24*, 379 (1973).
[9] Porter, R. N.: Ann. Rev. Phys. Chem. *25*, 317 (1974) and references therein.
[10] Gear, C. W.: J. Siam Num. Anal. *2B*, 69 (1964).
[11] Gear, C. W.: Numerical initial value problems in ordinary differential equations. Prentice-Hall 1971.
[12] Brumer, P., Thesis: Harvard University 1972.
[13] Marcus, R. A., in: Chemische Elementarprozesse (ed. Hartmann). Berlin-Heidelberg-New York: Springer 1968 and references therein.
[14] Robinson, P. J., Holbrook, K. A.: Unimolecular reactions. Wiley 1972.
[15] Forst, W.: Theory of unimolecular reactions. Acad. Press 1973.
[16] Present, R. D.: Kinetic theory of gases. McGraw-Hill 1958.
[17] Benson, S. W.: The foundations of chemical kinetics. McGraw-Hill 1960.
[18] Rice, O. K., in: Energy transfer in gases. 12th Solvay Congress. Interscience Pub. 1962.
[19] Laidler, K. J.: Chemical kinetics. McGraw-Hill 1965.
[20] Bunker, D. L.: Theory of elementary gas reaction rates. Pergamon Press 1966.
[21] Benson, S. W.: Thermochemical kinetics. Wiley 1968.
[22] Troe, J., Wagner, H. G.: Ann. Rev. Phys. Chem. *23*, 311 (1972).
[23] Westenberg, A. A.: Ann. Rev. Phys. Chem. *24*, 77 (1973).
[24] Farrar, J. M., Lee, Y. T.: Ann. Rev. Phys. Chem. *25*, 357 (1974) and references therein.
[25] Herschbach, D. R.: Disc. Faraday Soc. *33*, 149 (1962).
[26] Ross, J., Greene, E. F., in: Energy transfer in gases. 12th Solvay Congress. Interscience Pub. 1962.
[27] Toennies, J. P., in: Chemische Elementarprozesse (ed. Hartmann). Springer-Verlag 1968.
[28] Ramsay, N. R.: Molecular beams. Clarendon Press 1969.
[29] Kinsey, J. L.: Reaction kinetics (ed. Polanyi). M.T.P. Int. Rev. Sci. Med. Tech. Publ. Butterworth 1972.
[30] Toennies, J. P.: Physical chemistry, an advanced treatise, kinetics of gas reactions *4*. Acad. Press 1973.
[31] Molecular beam scattering. Disc. Faraday Soc. *55* (1973).
[32] Toennies, J. P.: Centenary lecture. Chem. Soc. Rev. *3*, 407 (1974).
[33] Carrington, T., Polanyi J. C.: Reaction kinetics (ed. Polanyi). MTP Int. Rev. Sci. Med. Tech. Publ. Butterworth 1972.
[34] Reactions of small molecules in excited states. Disc. Faraday Soc. *53* (1972).
[35] Levine, R. D.: Theoretical chemistry (ed. Brown). MTP Int. Rev. Sci. Med. Tech. Publ. Butterworth 1972.
[36] George, T. F., Ross, J.: Ann. Rev. Phys. Chem. *24*, 263 (1973).
[37] Bennewitz, H. G., Haerten, R., Müller, G.: Z. Phys. *226* 136 (1969).
[38] Bennewitz, H. G., Gengenbach, R., Haerten, R., Müller, G.: Z. Phys. *226*, 279 (1969).
[39] Bennewitz, H. G., Haerten, R.: Z. Phys. *227*, 399 (1969).
[40] Stolte, S., Reuss, J., Schwartz, H. L.: Abst. VII Int. Conf. Phys. Electronic At. Coll. North-Holland 1971.
[41] Moerkerken, H., Reuss, J.: same Ref. as[40].
[42] Beuhter, R. J., Bernstein, R. B., Kramer, K. H.: J. Amer. Chem. Soc. *88*, 5331 (1966).

43) Beuhter, R. J., Bernstein, R. B.: J. Chem. Phys. *51*, 5305 (1969).
44) Brooks, P. R.: Disc. Faraday Soc. *55*, 299 (1973).
45) Bernstein, R. B., Rulis, A. M.: Disc. Faraday Soc. *55*, 293 (1973).
46) Parson, J. M., Shobatake, K., Lee, Y. T., Rice, S. A.: Disc. Faraday Soc. *55*, 344 (1973).
47) Schafer, T. P., Siska, P. E., Parson, J. M., Tully, F. P., Wong, Y. C., Lee, Y. T.: J. Chem. Phys. *53*, 3385 (1970).
48) Schafer, T. P., Thesis: University of Chicago 1972.
49) McDonald, J. D., Lebreton, P. R., Lee, Y. T., Herschbach, D. R.: J. Chem. Phys. *56*, 769 (1972).
50) Miller, W. B., Safron, S. A., Herschbach, D. R.: J. Chem. Phys. *56*, 3581 (1972).
51) Maltz, C., Weinstein, N. O., Herschbach, D. R.: Mol. Phys. *24*, 133 (1972).
52) Hsu, D. S., Herschbach, D. R.: Disc. Faraday Soc. *55*, 116 (1973).
53) Cheung, J. T., McDonald, J. D., Herschbach, D. R.: Disc. Faraday Soc. *55*, 377 (1973).
54) Moore, C. B., Zittel, P. F.: Ann. Rev. Phys. Chem. *22*, 387 (1971).
55) Moore, C. B.: Science *182*, 541 (1973).
56) Schultz, A., Cruse, H. W., Zare, R. N.: J. Chem. Phys. *57*, 1354 (1972).
57) Dagdigian, P. J., Cruse, H. W., Zare, R. N.: J. Chem. Phys. *62*, 1824 (1975).
58) Cruse, H. W., Dagdigian, P. J., Zare, R. N.: Disc. Faraday Soc. *55*, 277 (1973).
59) Polanyi, J. C.: J. Chem. Phys. *34*, 347 (1961).
60) Polanyi, J. C., Woodall, K. B.: J. Chem. Phys. *56*, 1563 (1972).
61) Anlauf, K. G., Horne, D. S., McDonald, R. G., Polanyi, J. C., Woodall, K. B.: J. Chem. Phys. *57*, 1561 (1972).
62) Polanyi, J. C., Sloan, J. J.: J. Chem. Phys. *57*, 4988 (1972).
63) Hancock, G., Morley, C., Smith, I. W.: Chem. Phys. Lett. *12*, 193 (1971).
64) Freund, S. M., Fisk, G. A., Herschbach, D. R., Klemperer, W.: J. Chem. Phys. *54*, 2510 (1971).
65) Riley, S. J., Herschbach, D. R.: J. Chem. Phys. *53*, 3453 (1970).
66) Mariella, R. P., Herschbach, D. R., Klemperer, W.: J. Chem. Phys. *58*, 3785 (1973).
67) Bennewitz, H. G., Haerten, R., Müller, G.: Chem. Phys. Lett. *12*, 335 (1971).
68) Kasper, J. V., Pimentel, G. C.: Phys. Rev. Lett. *14*, 352 (1965).
69) Parker, H. J., Pimentel, G. C.: J. Chem. Phys. *51*, 91 (1969).
70) Berry, M. J., Pimentel, G. C.: J. Chem. Phys. *53*, 3453 (1970).
71) Coombe, R. D., Pimentel, G. C.: J. Chem. Phys. *59*, 1535 (1973).
72) Molina, M. J., Pimentel, G. C.: IEEE J. Quantum Electron. *9*, 64 (1973).
73) Airey, J. R.: IEEE J. Quantum Electron. *3*, 208 (1967).
74) Lin, M. C.: J. Phys. Chem. *75*, 3642 (1971).
75) King, D. L., Dixon, D. A., Herschbach, D. R.: J. Amer. Chem. Soc. *96*, 3328 (1974).
76) Dixon, D. A., Herschbach, D. R.: J. Amer. Chem. Soc. *97*, 6268 (1975).
77) Muckerman, J. T.: J. Chem. Phys. *56*, 2997 (1972).
78) Blais, N. C., Truhlar, D. G.: J. Chem. Phys. *58*, 1090 (1973).
79) Wilkins, R. L.: J. Chem. Phys. *58*, 3038 (1973).
80) Schatz, G. C., Bowman, J. M., Kuppermann, A.: J. Chem. Phys. *58*, 4023 (1973).
81) Jonathan, N., Melliar-Smith, C. M., Slater, D. H.: Mol. Phys. *20*, 93 (1971).
82) Laidler, K., Polanyi, J. C.: Progr. React. Kinet. *3*, 1 (1965).
83) Polanyi, J. C., Schreiber, J. L.: Kinetics in gas reactions (ed. Eyring), Vol. 6. Acad. Press 1973.
84) Eyring, H., Polanyi, M.: Z. Phys. Chem. B. *12*, 279 1931.
85) Hirschfelder, J. O., Eyring, H., Topley, B.: J. Chem. Phys. *4*, 170 (1936).
86) Evans, M. G., Polanyi, M.: Trans. Faraday Soc. *35*, 178 (1939).
87) Wall, F. T., Hiller, L. A., Mazur, J.: J. Chem. Phys. *29*, 255 (1958).
88) Wall, F. T., Hiller, L. A., Mazur, J.: J. Chem. Phys. *35*, 1284 (1961).
89) Wall, F. T., Porter, R. N.: J. Chem. Phys. *36*, 3256 (1962).
90) Wall, F. T., Porter, R. N.: J. Chem. Phys. *39*, 3112 (1963).
91) Blais, N. C., Bunker, D. L.: J. Chem. Phys. *36*, 2713 (1962).
92) Blais, N. C., Bunker, D. L.: J. Chem. Phys. *39*, 315 (1963).

93) Bunker, D. L., Blais, N. C.: J. Chem. Phys. *41*, 2377 (1964).
94) Polanyi, J. C., Rosner, S. O.: J. Chem. Phys. *38*, 1028 (1963).
95) Kuntz, P. J., Nemeth, E. M., Polanyi, J. C., Rosner, S. D.: J. Chem. Phys. *44*, 1168 (1966).
96) Polanyi, J. C.: Acc. Chem. Res. *5*, 161 (1972).
97) Karplus, M., Porter, R. N., Sharma, R. D.: J. Chem. Phys. *40*, 2033 (1964).
98) Porter, R. N., Karplus, M.: J. Chem. Phys. *40*, 1105 (1964).
99) Karplus, M., Raff, L. M.: J. Chem. Phys. *41*, 1267 (1964).
100) Raff, L. M., Karplus, M.: J. Chem. Phys. *44*, 1212 (1966).
101) Karplus, M., Porter, R. N., Sharma, R. D.: J. Chem. Phys. *43*, 3259 (1965).
102) Polanyi, J. C., Wong, W. H.: J. Chem. Phys. *51*, 1439 (1969).
103) Mok, M. H., Polanyi, J. C.: J. Chem. Phys. *51*, 1451 (1969).
104) Bunker, D. L., Goring, E. A.: Chem. Phys. Lett. *15*, 521 (1972).
105) Harris, R. M., Herschbach, D. R.: Disc. Faraday Soc. *55*, 121 (1973).
106) Bunker, D. L., Blais, N. C.: J. Chem. Phys. *37*, 2713 (1962).
107) Mok, M. H., Polanyi, J. C.: J. Chem. Phys. *53*, 4588 (1970).
108) Morokuma, K., Pedersen, L., Karplus, M.: J. Amer. Chem. Soc. *89*, 5064 (1967).
109) Porter, R. N., Thompson, D. L., Sims, L. B., Raff, L. M.: J. Amer. Chem. Soc. *92*, 3208 (1970).
110) Jaffe, S. B., Anderson, J. B.: J. Chem. Phys. *49*, 2859 (1968).
111) Jaffe, S. B., Anderson, J. B.: J. Chem. Phys. *51*, 1057 (1969).
112) Brumer, P., Karplus, M.: J. Chem. Phys. *58*, 3903 (1973).
113) Brumer, P., Karplus, M.: Faraday Disc. Chem. Soc. *55*, 80 (1973).
114) Loughlin, D. R., Thompson, D. L.: J. Chem. Phys. *59*, 4393 (1973).
115) Montrolland, E. W., Shuler, K. E.: Adv. Chem. Phys. *1*, 361 (1958).
116) Shuler, K. E., in: Chemische Elementarprozesse (ed. Hartmann). Springer-Verlag 1968 and references therein.
117) Ross, J., Mazur, P.: J. Chem. Phys. *35*, 19 (1961).
118) Eliason, M. A., Hirschfelder, J. O.: J. Chem. Phys. *30*, 1426 (1959).
119) Eyring, H. J., Hirschfelder, J. O., Taylor, H. S.: J. Chem. Phys. *4*, 479 (1936).
120) Gioumousis, G., Stevenson, D. P.: J. Chem. Phys. *29*, 294 (1958).
121) Broida, H. P., Polanyi, J. C., Callear, A. B., Zare, R. N., Herschbach, D. R., in: Chemical lasers. Appl. Opt. Suppl. *2* (1965).
122) Shuler, K. E., Carrington, T., Broida, H. P.: same Ref. as[121].
123) Adv. Chem. Phys. *10*: Molecular beams (ed. J. Ross). Interscience Publ. 1965.
124) Secrest, D.: J. Chem. Phys. *62*, 710 (1975).
125) Takayanagi, K.: Suppl. Prog. Theoret. Phys. *25*, 1 (1963).
126) Takayanagi, K.: Adv. At. Molec. Phys. *1*, 149 (1965).
127) Rapp, D., Kassal, T.: Chem. Rev. *69*, 61 (1969).
128) Gordon, R. G.: Meth. Comp. Phys. *10* (1971).
129) Connor, J. N., in: Ann. Rep. A Chem. Soc. (1973) and references therein.
130) Quantum theory (ed. Bates), Vol. I. Acad. Press 1961.
131) Wu, T. Y., Ohmura, T.: Quantum theory of scattering. Prentice Hall 1962.
132) Rodberg, L. S., Thaler, R. M.: Introduction to the quantum theory of scattering. Acad. Press 1967.
133) Herzfeld, K. F., Litowitz, T. A.: Absorption and dispersion of ultrasonic waves. Acad. Press 1959.
134) Cottrell, T. L., McCoubrey, J. C.: Molecular energy transfer in gases. Butterworth 1961.
135) Johnston, H. S.: Gas phase reaction rate theory, Ronald Press 1966.
136) Levine, R. D.: Quantum mechanics of molecular rate processes. Clarendon Press.1969.
137) Rapp, D.: Quantum mechanics. Holt 1971.
138) Child, M. S.: Molecular collision theory. Acad. Press 1974.
139) Levine, R. D., Berstein, R. B.: Molecular reaction dynamics. Clarendon Press 1974.
140) Wolken, G., Karplus, M.: J. Chem. Phys. *60*, 351 (1974).
141) Bowman, J. M., Kuppermann, A.: Chem. Phys. Lett. *12*, 1 (1971).
142) Diestler, D. J., Karplus, M.: J. Chem. Phys. *55*, 5832 (1971).
143) Fong, K. P., Diestler, D. J.: J. Chem. Phys. *56*, 3200 (1972).

144) Marcus, R. A.: Chem. Phys. Lett. *7*, 525 (1970).
145) Miller, W. H.: J. Chem. Phys. *53*, 1949 (1970).
146) Miller, M. H.: J. Chem. Phys. *54*, 5386 (1971).
147) Doll, J. D., George, T. F., Miller, W. H.: J. Chem. Phys. *58*, 1343 (1973).
148) Miller, W. H.: Acc. Chem. Res. *4*, 161 (1971).
149) Miller, W. H.: Adv. Chem. Phys. *25* (1974), and references therein.
150) Light, J. C.: Meth. Comp. Phys. *10* (1971) and references therein.
151) McCullough, E. A., Wyatt, R. E.: J. Chem. Phys. *54*, 3578 (1971).
152) McCullough, E. A., Wyatt, R. E.: J. Chem. Phys. *54*, 3592 (1971).
153) Dugan, J. V., Magee, J. L.: Adv. Chem. Phys. *21*, 207 (1971).
154) La Budde, R. A., Kuntz, P. J., Bernstein, R. B., Levine, R. D.: Chem. Phys. Lett. *19*, 7 (1973).
155) La Budde, R. A., Kuntz, P. J., Bernstein, R. B., Levine, R. D.: J. Chem. Phys. *59*, 6286 (1973).
156) George, T. F., Suplinskas, R. J.: J. Chem. Phys. *51*, 3666 (1969).
157) George, T. F., Suplinskas, R. J.: J. Chem. Phys. *54*, 1037 (1971).
158) George, T. F., Suplinskas, R. J.: J. Chem. Phys. *54*, 1046 (1971).
159) Dugan, J. V., Magee, J. L.: J. Chem. Phys. *58*, 5816 (1973).
160) Pattengill, M. D., Polanyi, J. C.: Chem. Phys. *3*, 1 (1974).
161) Herzfeld, K. F.: J. Chem. Phys. *47*, 743 (1967).
162) Raff, L. M.: J. Chem. Phys. *46*, 520 (1967).
163) Raff, L. M.: J. Chem. Phys. *47*, 1884 (1967).
164) Thommarson, R. L., Berend, G. C.: Int. J. Chem. Kinet. *5*, 629 (1973).
165) Berend, G. C., Thommarson, R. L.: J. Chem. Phys. *58*, 3203 (1973).
166) Berend, G. C., Thommarson, R. L.: J. Chem. Phys. *58*, 3454 (1973).
167) Wilkins, R. L.: J. Chem. Phys. *59*, 698 (1973).
168) Lester, W. A.: J. Chem. Phys. *53*, 1511 (1970).
169) Lester, W. A., Schaefer, J.: J. Chem. Phys. *59*, 3676 (1973).
170) La Budde, R. A., Bernstein, R. B.: J. Chem. Phys. *55*, 5499 (1971).
171) La Budde, R. A., Bernstein, R. B.: J. Chem. Phys. *59*, 3687 (1973).
172) Perry, D. S., Polanyi, J. C.: Can. J. Chem. *50*, 3916 (1972).
173) Douglas, D. J., Polanyi, J. C., Sloan, J. J.: J. Chem. Phys. *59*, 6679 (1973).
174) Perry, D. S., Polanyi, J. C., Wilson, C. W.: Chem. Phys. *3*, 317 (1974).
175) Karplus, M., Porter, R. N.: Disc. Faraday Soc. *44*, 164 (1967).
176) Godfrey, M., Karplus, M.: J. Chem. Phys. *49*, 3602 (1968).
177) Porter, R. N., Kunt, S.: J. Chem. Phys. *52*, 3240 (1970).
178) Brumer, P., Karplus, M.: J. Chem. Phys. *54*, 4955 (1971).
179) Porter, R. N., Sims, L. B., Thompson, D. L., Raff, L. M.: J. Chem. Phys. *58*, 2855 (1973).
180) Anderson, J. B.: J. Chem. Phys. *52*, 3849 (1970).
181) Wilkins, R. L.: J. Chem. Phys. *57*, 912 (1972).
182) Wilkins, R. L.: J. Chem. Phys. *58*, 2326 (1973).
183) Muckerman, J. T.: J. Chem. Phys. *54*, 1155 (1971).
184) Muckerman, J. T., Newton, M. D.: J. Chem. Phys. *56*, 3191 (1972).
185) Muckerman, J. T.: J. Chem. Phys. *57*, 3388 (1972).
186) Landau, L.: Phys. Z. Sow. *2*, 46 (1932).
187) Zener, C.: Proc. Roy. Soc. *A137*, 696 (1932).
188) Nikitin, E. E., in: Chemische Elementarprozesse (ed. Hartmann). Springer-Verlag 1968.
189) Blais, N.: J. Chem. Phys. *49*, 9 (1968).
190) Maier, W. B.: J. Chem. Phys. *54*, 2732 (1971).
191) Tully, J. C., Preston, R. K.: J. Chem. Phys. *55*, 562 (1971).
192) Warshel, A., Karplus, M.: Chem. Phys. Lett. *32*, 11 (1975).
193) Morokuma, K., George, T. F.: J. Chem. Phys. *59*, 1959 (1973).
194) George, T. F., Morokuma, K.: Chem. Phys. *2*, 129 (1973).
195) Jaffe, R. L., George, T. F., Morokuma, K.: Mol. Phys. *28*, 1489 (1974).
196) Jaffe, R. L., Morokuma, K., George, T. F.: J. Chem. Phys. *63*, 3417 (1975).

[197] Unpublished report on the: Workshop on reactions involving two surfaces. Orsay 1975.
[198] Shui, V. H.: J. Chem. Phys. *56*, 4266 (1972).
[199] Shui, V. H., Appleton, J. P., Keck, J. C.: J. Chem. Phys. *57*, 1704 (1972).
[200] Shui, V. H.: J. Chem. Phys. *58*, 4868 (1973).
[201] Clarke, A. G., Burns, G.: J. Chem. Phys. *55*, 4717 (1971).
[202] Clarke, A. G., Burns, G.: J. Chem. Phys. *56*, 4636 (1972).
[203] Clarke, A. G., Burns, G.: J. Chem. Phys. *58*, 1908 (1973).
[204] Wong, W. H., Burns, G.: J. Chem. Phys. *58*, 4454 (1973).
[205] Gelb, A., Kapral, R., Burns, G.: J. Chem. Phys. *59*, 2980 (1973).
[206] Borne, T. B., Bunker, D. L.: J. Chem. Phys. *55*, 4861 (1971).
[207] Kwei, G. H., Boffardi, B. D., Sun, S. F.: J. Chem. Phys. *58*, 1722 (1973).
[208] Roach, A. C., Child, M. S.: Mol. Phys. *14*, 1 (1968).
[209] Bunker, D. L.: J. Chem. Phys. *37*, 393 (1962).
[210] Bunker, D. L.: J. Chem. Phys. *40*, 1946 (1964).
[211] Bunker, D. L., Pattengill, M. D.: J. Chem. Phys. *48*, 772 (1968).
[212] Bunker, D. L., Pattengill, M. D.: J. Chem. Phys. *53*, 3041 (1970).
[213] Bunker, D. L.: J. Chem. Phys. *57*, 332 (1972).
[214] Bunker, D. L., Hase, W. L.: J. Chem. Phys. *59*, 4621 (1973).
[215] Harris, H. H., Bunker, D. L.: Chem. Phys. Lett. *11*, 433 (1971).
[216] Schneider, F. W., Rabinovitch, B. S.: J. Amer. Chem. Soc. *84*, 4215 (1962).
[217] Ting, C. T., Rowland, F. S.: J. Phys. Chem. *74*, 4080 (1970).
[218] Raff, L. M.: J. Chem. Phys. *44*, 1202 (1966).
[219] Kuntz, P. J., Nemeth, E. M., Polanyi, J. C., Wong, W. H.: J. Chem. Phys. *52*, 4654 (1970).
[220] Bunker, D. L., Pattengill, M. D.: Chem. Phys. Lett. *4*, 315 (1969).
[221] Valencich, T., Bunker, D. L.: Chem. Phys. Lett. *20*, 50 (1973).
[222] Wang, I. S., Karplus, M.: J. Amer. Chem. Soc. *95*, 8160 (1973).
[223] Raff, L. M., Stivers, L., Porter, R. N., Thompson, D. L., Sims, L. B.: J. Chem. Phys. *52*, 3449 (1970).
[224] Porter, R. N., Tompson, D. L., Sims, L. B.: J. Amer. Chem. Soc. *92*, 3208 (1970).
[225] Raff, L. M., Tompson, D. L., Sims, L. B., Porter, R. N.: J. Chem. Phys. *56*, 5998 (1972).
[226] Spicer, L. D., Rabinovitch, B. S.: Ann. Rev. Phys. Chem. *21*, 349 (1970).
[227] Henry, J. M., Anderson, J. B., Jaffé, R. L.: Chem. Phys. Lett. *20*, 138 (1973).
[228] Sullivan, J. H.: J. Chem. Phys. *46*, 73 (1967).
[229] Gordon, R. G.: Disc. Faraday Soc. *55* (1973).
[230] Schlessinger, L.: Phys. Rev. *167*, 1411 (1968).
[231] Baker, G. A., Gammel, J. L. (eds.): The Pade approximant in theoretical physics. Acad. Press 1970.
[232] Wall, H. S.: The analytic theory of continued fractions. Van Nostrand 1948.
[233] Walsh, J. L., Ahlberg, J. H., Nilson, E. N.: J. Math. Mech. *11*, 225 (1962).
[234] Ahlberg, J. A., Nilson, E. N., Walsh, J. L.: The theory of splines and their applications. Acad. Press 1967.
[235] Schumaker, L. L.: Theory and applications of spline functions (ed. Greville). Acad. Press 1969.
[236] Sand, A., Weintraub, S.: A book of splines. Wiley 1971.
[237] Sathyamorthy, N., Raff, L. M.: J. Chem. Phys. *63*, 464 (1975).
[238] Bowman, J. M., Kuppermann, A.: Chem. Phys. Lett. *34*, 523 (1975).
[239] Dunfield, L. G., Read, J. F.: J. Chem. Phys. *57*, 2178 (1972).
[240] Gilbert, T. L., Bertoncini, P. J.: J. Chem. Phys. *61*, 3026 (1974).
[241] Gilbert, T. L., Bertoncini, P. J.: Chem. Phys. Lett. *29*, 569 (1974).
[242] Gilbert, T. L., Bertoncini, P. J.: J. Chem. Phys. *62*, 1289 (1975).
[243] Shore, B. W.: J. Chem. Phys. *59*, 6450 (1973).
[244] Horsley, J., Flouquet, F., Chapuisat, X.: Lect. 3rd Colloq. High Resol. Molec. Spectr. (1973).
[245] DeBoor, C.: J. Math. Phys. *41*, 212 (1962).
[246] Adv. Chem. Phys. XXI, Part. II: Kinetics in gas reactions (ed. Laidler).
[247] Salem, L.: J. Amer. Chem. Soc. *96*, 3486 (1974).

[248] Salem, L., Leforestier, C., Segal, G., Wetmore, R.: J. Amer. Chem. Soc. *97*, 479 (1975).
[249] Miller, W. H., George, T. F.: J. Chem. Phys. *56*, 5637 (1972).
[250] Goldstein, H.: Classical mechanics. Addison-Wesley 1959.
[251] Hammersley, J. M., Handscomb, D. C.: Monte-Carlo methods. Methuen 1954.
[252] Kahn, H.: Applications of Monte-Carlo. Rand Corporation Research Memorandum. RM-1237-AEC (1956).
[253] Sizun, M.: Thèse de 3e Cycle. Orsay 1972.
[254] Wigner, E.: Phys. Rev. *40*, 749 (1932).
[255] Fiquet-Fayard, F., Sizun, M., Goursaud, S.: J. de Physique *33*, 669 (1972).
[256] Flouquet, F., Horsley, J., Chapuisat, X.: to be published.
[257] Carrington, T.: J. Chem. Phys. *41*, 2012 (1964).
[258] Horie, T., Kasuga, T.: J. Chem. Phys. *40*, 1683 (1964).
[259] Trautz, M., Winkler, K.: J. prakt. Chem. 2 *104*, 53 (1922).
[260] Baldwin, J. E., Grayston, M. W.: J. Amer. Chem. Soc. *96*, 1629 and 1630 (1974).
[261] Rabinovitch, B. S., Schlag, E. W., Wiberg, K. W.: J. Chem. Phys. *28*, 504 (1958).
[262] Schlag, E. W., Rabinovitch, B. S.: J. Amer. Chem. Soc. *82*, 5996 (1960).
[263] Flowers, M. C., Frey, H. M.: Proc. Roy. Soc. A, *257*, 122 (1960).
[264] Flowers, M. C., Frey, H. M.: Proc. Roy. Soc. A, *260*, 424 (1961).
[265] Frey, H. M., Marshall, D. C.: J. Chem. Soc. 5717 (1963).
[266] Setser, D. W., Rabinovitch, B. S.: J. Amer. Chem. Soc. *86*, 564 (1964).
[267] Willcott III, M. R., Cargle, V. H.: J. Amer. Chem. Soc. *89*, 723 (1967).
[268] Crawford, R. J., Lynch, T. R.: Can. J. Chem. *46*, 1457 (1968).
[269] Berson, J. A., Balquist, J. M.: J. Amer. Chem. Soc. *90*, 7343 (1968).
[270] Carter, W. L., Bergman, R. G.: J. Amer. Chem. Soc. *90*, 7344 (1968).
[271] Bergman, R. G., Carter, W. L.: J. Amer. Chem. Soc. *91*, 7411 (1969).
[272] Willcott III, M. R., Cargle, V. H.: J. Amer. Chem. Soc. *91*, 4310 (1969).
[273] von Doering, W. E., Sachdev, K.: J. Amer. Chem. Soc. *96*, 1168 (1974).
[274] Berson, J. A., Pedersen, L. D., Carpenter, B. K.: J. Amer. Chem. Soc. *97*, 240 (1975).
[275] Berson, J. A., Pedersen, L. D.: J. Amer. Chem. Soc. *97*, 238 (1975).
[276] Bergman, R. G., in: Free radicals (ed. Kochi). Wiley 1973.
[277] Hoffmann, R.: J. Amer. Chem. Soc. *90*, 1475 (1968).
[278] Buenker, R. J., Peyerimhoff, S. D.: J. Phys. Chem. *73*, 1299 (1969).
[279] Siu, A. K. Q., St-John II, W. M., Hayes, E. F.: J. Amer. Chem. Soc. *92*, 7249 (1970).
[280] Hay, P. J., Hunt, W. J., Goddard, W. A., III: J. Amer. Chem. Soc. *94*, 638 (1972).
[281] Benson, S. W.: J. Chem. Phys. *34*, 521 (1961).
[282] Buchwalter, S. L., Closs, G. L.: J. Amer. Chem. Soc. *97*, 3857 (1975).
[283] Hehre, W. J., Stewart, R. F., Pople, J. A.: J. Chem. Phys. *51*, 2657 (1969).
[284] Wright, J. S., Tan, G., Laidler, K. J., Hulse, J. E.: Chem. Phys. Lett. *30*, 200 (1975).
[285] Chapuisat, X., Jean, Y., Salem, L.: Chem. Phys. Lett. *37*, 119 (1976).

Received December 23, 1975